

ผลของสารลดแรงตึงผิวและปริมาณของดินเหนียวปรับสภาพต่อสมบัติทางกลและสมบัติ
ในการสกัดกั้นการซึมผ่านก๊าซของฟิล์มนาโนคอมพอสิตของ
เอทิลีนไวนิลแอลกอฮอล์โคพอลิเมอร์และดินเหนียว



นางสาวงามแก้ว พจน์ไยธิน

สถาบันวิทยบริการ จุฬาลงกรณ์มหาวิทยาลัย

วิทยานิพนธ์นี้เป็นส่วนหนึ่งของการศึกษาตามหลักสูตรปริญญาวิศวกรรมศาสตรมหาบัณฑิต

สาขาวิชาวิศวกรรมเคมี ภาควิชาวิศวกรรมเคมี

คณะวิศวกรรมศาสตร์ จุฬาลงกรณ์มหาวิทยาลัย

ปีการศึกษา 2549

ลิขสิทธิ์ของจุฬาลงกรณ์มหาวิทยาลัย

EFFECT OF SURFACTANT AND ORGANOCLAY LOADING ON
MECHANICAL AND GAS BARRIER PROPERTIES OF EVOH/CLAY
NANOCOMPOSITE FILMS



Miss Khamkaew Photyotin

สถาบันวิทยบริการ
จุฬาลงกรณ์มหาวิทยาลัย

A Thesis Submitted in Partial Fulfillment of the Requirements
for the Degree of Master of Engineering Program in Chemical Engineering

Department of Chemical Engineering

Faculty of Engineering

Chulalongkorn University

Academic Year 2006

Copyright of Chulalongkorn University

Thesis Title EFFECT OF SURFACTANT AND ORGANOCCLAY LOADING
ON MECHANICAL AND GAS BARRIER PROPERTIES OF
EVOH/CLAY NANOCOMPOSITE FILMS

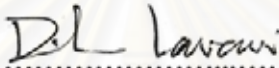
By Miss Khamkaew Photyotin

Field of Study Chemical Engineering

Thesis Advisor Anongnat Somwangthanaroj, Ph.D.


Thesis Co-advisor Sarintorn Limpanart, Ph.D.

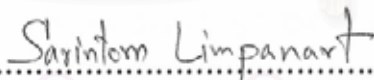
Accepted by the Faculty of Engineering, Chulalongkorn University in
Partial Fulfillment of the Requirement for the Master's Degree

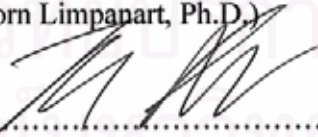

.....Dean of the Faculty of Engineering
(Professor Direk Lavansiri, Ph.D.)

THESIS COMMITTEE


.....Chairman
(Associate Professor Tawatchai Charinpanitkul, D.Eng.)


.....Thesis Advisor
(Anongnat Somwangthanaroj, Ph.D.)


.....Thesis Co-advisor
(Sarintorn Limpanart, Ph.D.)


.....Member
(Assistant Professor Toemsak Srikhirin, Ph.D.)

ขามแก้ว พจน์โยธิน: ผลของสารลดแรงตึงผิวและปริมาณของดินเหนียวปรับสภาพต่อสมบัติทางกลและสมบัติในการสกัดกั้นการซึมผ่านก๊าซของฟิล์มนาโนคอมพอสิตของเอทิลีน-ไวนิลแอลกอฮอล์โคพอลิเมอร์และดินเหนียว. (EFFECT OF SURFACTANT AND ORGANOCLAY LOADING ON MECHANICAL AND GAS BARRIER PROPERTIES OF EVOH/CLAY NANOCOMPOSITE FILMS) อ.ที่ปรึกษา: ดร.อนงค์นาฏ สมหวังธนโรจน์, อ.ที่ปรึกษาร่วม: ดร.สรินทร ลิมปนาท, 98 หน้า.

ฟิล์มนาโนคอมพอสิตมีคุณสมบัติในการสกัดกั้นการซึมผ่านของก๊าซที่ดีกว่าเมื่อเปรียบเทียบกับพอลิเมอร์บริสุทธิ์ เนื่องจากชั้นขีตึกของดินเหนียวที่กระจายตัวอยู่ในเนื้อพอลิเมอร์ จะทำหน้าที่เป็นตัวกีดขวางเส้นทางการเคลื่อนที่ของก๊าซออกซิเจน ในงานวิจัยนี้ ฟิล์มนาโนคอมพอสิตของเอทิลีนไวนิลแอลกอฮอล์โคพอลิเมอร์และดินเหนียวถูกเตรียมผ่านทางหัวฉีดเป่ากลางที่ต่อเชื่อมอยู่กับเครื่องอัดรีดสกรูคู่ เพื่อที่จะศึกษาสมบัติทางกล ทางความร้อน และสมบัติในการสกัดกั้นการซึมผ่านของก๊าซ โดยมีการปรับเปลี่ยนชนิดของสารลดแรงตึงผิวและปริมาณของดินเหนียวปรับสภาพ เนื่องจาก จำนวนอะตอมของคาร์บอนในสายโซ่อัลคิลและจำนวนหน่วยซ้ำของหมู่ออกซิเอทิลีนในโครงสร้างของสารลดแรงตึงผิว จะมีผลต่อการกระจายตัวของดินเหนียวในเนื้อเอทิลีนไวนิลแอลกอฮอล์โคพอลิเมอร์ ดังนั้น ในงานวิจัยนี้จะศึกษาสารลดแรงตึงผิว 6 ชนิด ซึ่งสามารถแบ่งได้เป็น 3 กลุ่มหลักๆ คือ กลุ่มของสารลดแรงตึงผิวที่มีสายโซ่อัลคิลสั้น (มีคาร์บอน 12 อะตอม) และที่มีสายโซ่อัลคิลยาว (มีคาร์บอน 18 อะตอม) กลุ่มของสารลดแรงตึงผิวที่มีหมู่แอลคิล 1 หมู่ และ 2 หมู่ และกลุ่มของสารลดแรงตึงผิวที่มีหน่วยซ้ำของหมู่ออกซิเอทิลีน 2 และ 15 หน่วย

จากการศึกษาพบว่า ฟิล์มนาโนคอมพอสิตของเอทิลีนไวนิลแอลกอฮอล์โคพอลิเมอร์และดินเหนียวที่ใช้สารลดแรงตึงผิวที่มีสายโซ่อัลคิลยาวหรือมีหน่วยซ้ำของหมู่ออกซิเอทิลีนจำนวนมาก จะให้ค่าความแข็งแรงและค่ามอดูลัสที่สูงกว่าสารลดแรงตึงผิวที่มีสายโซ่อัลคิลสั้น อย่างไรก็ตาม ฟิล์มนาโนคอมพอสิตที่ใช้สารลดแรงตึงผิวทั้ง 2 ชนิดจะมีคุณสมบัติทางความร้อนคล้ายกัน ส่วนฟิล์มนาโนคอมพอสิตที่ใช้สารลดแรงตึงผิวที่มีสายโซ่อัลคิลทางเดียวจะให้ค่าความแข็งแรง ค่ามอดูลัส และระยะยืดที่จุดขาดสูงกว่าสารลดแรงตึงผิวที่มีสายโซ่อัลคิล 2 ทาง และให้ค่าอุณหภูมิหลอมเหลวที่สูงกว่าสารลดแรงตึงผิวที่มีสายโซ่อัลคิล 2 ทางเล็กน้อย อย่างไรก็ตาม ฟิล์มนาโนคอมพอสิตของเอทิลีนไวนิลแอลกอฮอล์โคพอลิเมอร์และดินเหนียวจะสกัดกั้นการซึมผ่านก๊าซได้น้อยลงเล็กน้อยเมื่อเปรียบเทียบกับเอทิลีนไวนิลแอลกอฮอล์โคพอลิเมอร์บริสุทธิ์ ยกเว้น ฟิล์มที่ใช้สารลดแรงตึงผิวที่มีสายโซ่อัลคิล 2 ทาง ที่สกัดกั้นการซึมผ่านก๊าซได้มากขึ้น 2.59% นอกจากนี้ ที่ปริมาณของดินเหนียวปรับสภาพ 3% โดยน้ำหนักพบว่า ฟิล์มนาโนคอมพอสิตจะมีความแข็งแรงและมีค่ามอดูลัสสูงที่สุด และที่ 1% โดยน้ำหนักของดินเหนียวปรับสภาพ จะทำให้ฟิล์มนาโนคอมพอสิตมีระยะยืดที่จุดขาดดีที่สุด แต่ดีกว่าที่ 3% โดยน้ำหนักเพียง 4.88%

ภาควิชา.....วิศวกรรมเคมี.....ลายมือชื่อนิสิต..... ขามแก้ว พจน์โยธิน
สาขาวิชา.....วิศวกรรมเคมี.....ลายมือชื่ออาจารย์ที่ปรึกษา.....
ปีการศึกษา.....2549.....ลายมือชื่ออาจารย์ที่ปรึกษาร่วม.....

#4870235521: MAJOR CHEMICAL ENGINEERING

KEY WORDS: ETHYLENE VINYL ALCOHOL COPOLYMER/ CLAY/
NANOCOMPOSITES/ BARRIER PROPERTY

KHAMKAEW PHOTYOTIN: EFFECT OF SURFACTANT AND ORGANOCCLAY LOADING ON MECHANICAL AND GAS BARRIER PROPERTIES OF EVOH/CLAY NANOCOMPOSITE FILMS. THESIS ADVISOR: ANONGNAT SOMWANGTHANAROJ, Ph.D., THESIS CO-ADVISOR: SARINTORN LIMPANART, Ph.D., 98 pp.

Nanocomposite films exhibit good gas barrier properties, compared to pure polymer because the pathway of oxygen is obstructed by silicate layers of clay dispersed in polymer matrix. Consequently, nanocomposite films could be used in packaging application. In this study, EVOH/clay nanocomposite films were prepared via twin screw extruder attached to blown film die in order to study the mechanical, thermal and gas barrier properties by varying types of surfactant and the amount of organoclay loading. The number of carbon atoms in alkyl chain and the number of oxyethylene groups of surfactant structures had an influence on clay dispersion in EVOH matrix. Six surfactants, which were used in this study, were divided into 3 groups, i.e., short (C12) and long (C18) alkyl tail surfactant groups, one and two alkyl tail surfactant groups and 2 and 15 repeating units of oxyethylene surfactant groups.

Nanocomposite films, containing long alkyl chain or more repeating units of oxyethylene, showed higher tensile strength and tensile modulus than those with short alkyl chain surfactant. However, nanocomposite films containing both kinds of surfactants exhibited similar thermal properties. Nanocomposite films containing one alkyl tail surfactant showed higher tensile strength, tensile modulus and elongation at break than those with two alkyl tail surfactant. In addition, nanocomposites with one alkyl tail surfactant showed slightly higher melting temperature than those with two alkyl tails surfactant. The gas barrier property of EVOH/clay nanocomposite films slightly decreased compared to pure EVOH film except nanocomposite film with two alkyl tail surfactant (increased 2.59%). EVOH/clay nanocomposite films containing 3 wt% MMT_T organoclay showed the highest tensile strength and tensile modulus. In addition, the nanocomposite films containing 1 wt% MMT_T organoclay showed the highest elongation at break but it was only 4.88% better than those containing 3 wt% MMT_T organoclay.

Department.....Chemical Engineering..... Student's signature..... Khamkaew P.

Field of study.....Chemical Engineering..... Advisor's signature..... Anongnat Somwangthanaroj

Academic year.....2006..... Co-advisor's signature..... Sarintorn Limpant

ACKNOWLEDGMENTS

The author would like to express a sincere gratitude and deep appreciation to her advisor, Dr.Anongnat Somwangthanaroj, for her kindness, supervision, suggestion and encouragement throughout this work and to her co-advisor, Dr.Sirintorn Limpanart, for her encouragement and advice.

Gratefully thanks to Associate Professor Tawatchai Charinpanitkul and Assistant Professor Toemsak Srikirin for serving as the chairman and the member of the thesis committee, respectively, whose comments were constructive and substantial helpful.

Thankful to Mr.Srichalai Khunphon and his staff , Metallurgy and Materials Science Research Institute, Thailand, for their kindly support in the treatment of clay.

Thankful to Akzo Nobel, Arnhem, Kunimine Industrial Co.,Ltd., Japan and Kuraray Co.,Ltd., USA for their raw materials support. They support surfactant, clay and EVOH copolymers, respectively.

Furthermore, thankful to all member of Polymer Engineering Research Group from the Department of Chemical Engineering, Faculty of Engineering, Chulalongkorn University.

Finally, she would like to express a sincere gratitude to her parents for encouragement, understanding and support during her studies.

CONTENTS

	PAGE
ABSTRACT (IN THAI)	iv
ABSTRACT (IN ENGLISH)	v
ACKNOWLEDGEMENTS	vi
CONTENTS	vii
LIST OF TABLES	xi
LIST OF FIGURES	xiii
 CHAPTER	
I INTRODUCTION	1
1.1 General Introduction.....	1
1.2 Objectives of the Present Study.....	2
1.3 Scopes of the Present Study.....	3
 II THEORY	4
2.1 EVOH copolymers.....	4
2.2 Clay and Organoclay.....	6
2.2.1 Clays.....	6
2.2.2 Organoclay.....	7
2.3 Polymer/Clay Nanocomposites.....	8
2.3.1 The Methods for Polymer/Clay Nanocomposite Preparation.....	8
2.3.2 The Formation of Polymer/Clay Nanocomposite.....	9
2.4 EVOH/Clay Nanocomposites.....	10
2.5 Processing Techniques.....	11
2.5.1 Polymer extrusion.....	11
2.5.1.1 Twin screw extrusion.....	11
2.5.1.2 Blown film Extrusion.....	12

	PAGE
2.6 Characterizations.....	12
2.6.1 Mechanical Testing.....	12
2.6.2 X-ray Diffraction (XRD)	13
2.6.3 Differential Scanning Calorimetry (DSC)	15
2.6.4 Oxygen Transmission Rate (O ₂ TR)	16
III LITERATURE REVIEWS.....	17
IV EXPERIMENTS.....	25
4.1 Materials.....	25
4.2 Preparation of the organoclay.....	27
4.3 Preparation of EVOH/clay nanocomposites by melt processing.....	28
4.4 Characterizations.....	29
4.4.1 X-ray Diffraction (XRD)	29
4.4.2 Mechanical Testing.....	29
4.4.3 Differential Scanning Calorimetry (DSC)	30
4.4.4 Oxygen Transmission Rate (O ₂ TR)	30
V RESULTS AND DISCUSSION.....	31
5.1 Effect of surfactant types on EVOH/clay nanocomposite films’ Properties.....	31
5.1.1 Degree of clay dispersion of EVOH/clay nanocomposite films.....	32
5.1.1.1 Effect of the short (C12) and long (C18) alkyl tail surfactant.....	35
5.1.1.2 Effect of the number of repeating units of oxyethylene.....	37
5.1.1.3 Effect of the number of alkyl tail surfactant.....	38
5.1.1.4 Degree of crystallinity of EVOH/clay nanocomposite Films.....	40

	PAGE
5.1.2 Thermal properties of EVOH/clay nanocomposite films.....	42
5.1.3 The mechanical properties of EVOH/clay nanocomposite films.....	45
5.1.3.1 Effect of the short (C12) and long (C18) alkyl tail surfactant.....	45
5.1.3.2 Effect of the number of repeating units of oxyethylene.....	49
5.1.3.3 Effect of the number of alkyl tail surfactant.....	50
5.1.4 The oxygen transmission rate (O ₂ TR) of EVOH/clay nanocomposite films.....	53
5.2 Effect of organoclay loading on EVOH/clay nanocomposite films Properties.....	55
5.2.1 Degree of clay dispersion and degree of crystallinity of EVOH/clay nanocomposite films.....	55
5.2.2 Thermal properties of EVOH/clay nanocomposite films.....	58
5.2.3 The mechanical properties of EVOH/clay nanocomposite films.....	61
5.2.4 The oxygen transmission rate (O ₂ TR) of EVOH/clay nanocomposite films.....	64
VI CONCLUSIONS.....	65
REFERENCES.....	67
APPENDICES.....	70
Appendix A Determination of surfactant loading.....	71
Appendix B Calculation of interlayer spacing of silicate layers of clay.....	72
Appendix C Inorganic content of clay and organoclays.....	75
Appendix D Inorganic content of EVOH/clay nanocomposites at different organoclay loading.....	76
Appendix E The crystalline-melting temperature (T _m) and the crystallization temperature (T _c).....	77
Appendix F Percent of crystallinity calculation.....	83
Appendix G The mechanical properties of EVOH/clay nanocomposites.....	87

	PAGE
Appendix H The oxygen transmission rate (O_2TR) of EVOH/clay nanocomposite films.....	97
VITAE	98



สถาบันวิทยบริการ
จุฬาลงกรณ์มหาวิทยาลัย

LIST OF TABLES

TABLE	PAGE
2.1 The oxygen gas transmission rate of various grades of EVOH copolymers.....	5
2.2 Barrier properties comparison of various polymers.....	6
5.1 The relationship between the degree of clay dispersion in EVOH matrix and the oxygen transmission rate of EVOH/clay nanocomposite films containing 3 wt% different organoclays.....	54
B.1 The degree of clay dispersion of organoclays and EVOH/clay nanocomposites.....	73
B.2 The degree of clay dispersion of EVOH/clay nanocomposite films containing different MMT_T organoclay loading.....	74
C.1 Inorganic content and surfactant content of clay and organoclays.....	75
D.1 Inorganic content of EVOH/Clay nanocomposites containing MMT_T at different organoclay loading.....	76
E.1 The crystalline-melting temperature (T_m) of EVOH/clay nanocomposite films containing 3 wt% organoclay, which was treated by different surfactant.....	77
E.2 The crystallization temperature (T_c) of EVOH/clay nanocomposite films containing 3 wt% organoclay, which was treated by different surfactant.....	77
E.3 T_m and T_c of EVOH/clay nanocomposite films containing different MMT_T organoclay loading.....	78
F.1 The relative degree of crystallinity of EVOH/clay nanocomposite films containing different surfactants, which were determined by XRD.....	85
F.2 The relative degree of crystallinity of EVOH/clay nanocomposite films containing different MMT_T organoclay loadings, which were determined by XRD.....	85
F.3 The relative degree of crystallinity of EVOH/clay nanocomposite films containing different surfactants, which were determined by DSC.....	86

TABLE	PAGE
F.4 The relative degree of crystallinity of EVOH/clay nanocomposite films containing different MMT_T organoclay loadings, which were determined by DSC.....	86
G.1 Tensile strength of pure EVOH.....	87
G.2 Tensile strength of EVOH/clay nanocomposite films containing 3 wt% MMT_C12/2 organoclay.....	88
G.3 Tensile strength of EVOH/clay nanocomposite films containing 3 wt% MMT_C18/2 organoclay.....	89
G.4 Tensile strength of EVOH/clay nanocomposite films containing 3 wt% MMT_2HT organoclay.....	90
G.5 Tensile strength of EVOH/clay nanocomposite films containing 3 wt% MMT_C12/15 organoclay.....	91
G.6 Tensile strength of EVOH/clay nanocomposite films containing 3 wt% MMT_C18/15 organoclay.....	92
G.7 Tensile strength of EVOH/clay nanocomposite films containing 1 wt% MMT_T organoclay.....	93
G.8 Tensile strength of EVOH/clay nanocomposite films containing 3 wt% MMT_T organoclay.....	94
G.9 Tensile strength of EVOH/clay nanocomposite films containing 5 wt% MMT_T organoclay.....	95
G.10 Tensile strength of EVOH/clay nanocomposite films containing 7 wt% MMT_T organoclay.....	96
H.1 Oxygen transmission rate of EVOH/clay nanocomposite films containing 3 wt% organoclays, which were treated with different surfactants, at 23°C, 1 atm and 0 % R.H.....	97
H.2 Oxygen transmission rate of EVOH/clay nanocomposite films containing MMT_T were prepared with different organoclay loadings (1, 3, 5 and 7 wt% organoclay), at 23°C, 1 atm and 0 % R.H.....	97

LIST OF FIGURES

FIGURE	PAGE
2.1 The structure of EVOH copolymers.....	4
2.2 The crystal structure of montmorillonite or bentonite.....	7
2.3 The treatment of clay by ion exchange with organic cation.....	8
2.4 The formation of polymer/clay nanocomposite.....	10
2.5 Schematic of a twin screw extruder.....	11
2.6 Diagram of a blown film extrusion line.....	12
2.7 Diagram of stress/strain of sample under tension.....	13
2.8 X-ray diffractometer (D8 advance BRUKER German)	14
2.9 Diagram of X-ray diffraction analysis.....	14
2.10 Oxygen gas transmission apparatus.....	16
3.1 The molecular structure of three surfactants were used as examples $M_1H_1(HT)_2$ is Methyl bis(hydrogenated-tallow) ammonium montmorillonite $M_1T_1(HE)_2$ is Bis(2-hydroxy-ethyl)methyl tallow ammonium montmorillonite $M_2H_1(HT)_1$ is Dimethyl hydrogenated-tallow ammonium montmorillonite.....	18
3.2 WAXS results for $M_1H_1(HT)_2$, $M_1T_1(HE)_2$ and $M_2H_1(HT)_1$ organoclay and pristine clay (NaMMT)	18
3.3 XRD curves of organoclay and PP/EPDM nanocomposites at various clay loading (3, 5 and 7 wt%) and 3 wt% with 0.5 phr compatibilizer.....	19
3.4 Tensile modulus of polyamide 6/clay nanocomposites at different clay loading (wt%).....	20
3.5 Yield strength and strain at yield of polyamide 6/clay nanocomposites at different clay loading (wt%).....	21
3.6 DSC heating curve for PP/EPDM blend without nanoclay (solid line) and with 3 wt% clay (dashed line)	22
3.7 Melting temperature and heat of melting of poly(ethylene oxide)/clay nanocomposites at various organoclay loading.....	23
3.8 Modulus of EVOH/clay nanocomposites, which consisted of 3 wt% clay, at various percent of relative humidity.....	24

FIGURE	PAGE
4.1 Octadecylmethyl[polyoxyethylene (15)] ammonium chloride (Ethoquad 18/25)	25
4.2 Cocoalkylmethyl[polyoxyethylene (15)] ammonium chloride (Ethoquad C/25)	26
4.3 Cocoalkylmethylbis(2-hydroxyethyl) ammonium chloride (Ethoquad C/12-75)	26
4.4 Oleylmethylbis(2-hydroxyethyl) ammonium chloride (Ethoquad O/12 PG).....	26
4.5 Trimethyl tallow quaternary ammonium chloride (Arquad T-50)	27
4.6 Dimethyl bis(hydrogenated-tallow) ammonium chloride (Arquad 2HT-75).....	27
4.7 Tensile test sample.....	29
5.1 X-ray diffraction patterns of pristine clay and organoclays, which were treated by different surfactant: C18/2, T, 2HT, C12/15 and C18/15, at $2\theta = 1-10^\circ$	33
5.2 X-ray diffraction patterns of EVOH/clay nanocomposite films containing 3 wt% organoclays, which were treated with different surfactant types at $2\theta = 1-10^\circ$	34
5.3 X-ray diffraction patterns of organoclays and EVOH/clay nanocomposite films containing 3 wt% MMT_C12/15 and MMT_C18/15 organoclays, at $2\theta = 1-10^\circ$	35
5.4 X-ray diffraction patterns of EVOH/clay nanocomposite films containing 3 wt% MMT_C12/2 and MMT_C12/15 organoclays.....	37
5.5 X-ray diffraction patterns of organoclays and EVOH/clay nanocomposite films containing 3 wt% MMT_T and MMT_2HT organoclays.....	39
5.6 X-ray diffraction patterns of EVOH/clay nanocomposite films containing 3 wt% organoclays, which were treated with different surfactant types, at $2\theta = 17-24^\circ$	41
5.7 DSC melting curves of EVOH/clay nanocomposite films containing 3 wt% organoclays, which were treated with different surfactant types, at heating rate of $10^\circ\text{C}/\text{min}$	43

FIGURE	PAGE
5.8 DSC cooling curves of EVOH/clay nanocomposite films containing 3 wt% organoclays, which were treated with different surfactant types, at cooling rate of 10°C/min.....	44
5.9 Tensile strength of EVOH/clay nanocomposite films containing 3 wt% MMT_C12/2, MMT_C12/15, MMT_C18/2 and MMT_C18/15 organoclays ..	46
5.10 Tensile modulus of EVOH/clay nanocomposite films containing 3 wt% MMT_C12/2, MMT_C12/15, MMT_C18/2 and MMT_C18/15 organoclays ..	47
5.11 Elongation at break of EVOH/clay nanocomposite films containing 3 wt% MMT_C12/2, MMT_C12/15, MMT_C18/2 and MMT_C18/15 organoclays ..	48
5.12 Tensile strength of EVOH/clay nanocomposite films containing 3 wt% MMT_T and MMT_2HT organoclays.....	50
5.13 Tensile modulus of EVOH/clay nanocomposite films containing 3 wt% MMT_T and MMT_2HT organoclays.....	51
5.14 Elongation at break of EVOH/clay nanocomposite films containing 3 wt% MMT_T and MMT_2HT organoclays.....	52
5.15 Oxygen transmission rate of EVOH/clay nanocomposite films containing 3 wt% organoclays, 23°C, 1 atm and 0 % RH.....	53
5.16 X-ray diffraction patterns of EVOH/clay nanocomposite films with different MMT_T organoclay loading, at $2\theta = 1-10^\circ$	56
5.17 X-ray diffraction patterns of EVOH/clay nanocomposite films with different MMT_T organoclay loadings, at $2\theta = 17-24^\circ$	57
5.18 DSC melting curves of EVOH/clay nanocomposite films containing MMT_T organoclay, at heating rate of 10°C/min.....	59
5.19 DSC cooling curves of EVOH/clay nanocomposite films containing MMT_T organoclay, at cooling rate of 10°C/min.....	60
5.20 Tensile strength and elongation at break of EVOH/clay nanocomposite films containing different MMT_T organoclay loading.....	62
5.21 Tensile modulus of EVOH/clay nanocomposite films containing different MMT_T organoclay loading.....	63
5.22 Oxygen transmission rate of EVOH/clay nanocomposite films containing different MMT_T organoclay loading, at 23°C, 1 atm and 0 % RH.....	64

FIGURE	PAGE
E.1 DSC cooling curves of EVOH/clay nanocomposite films containing 3 wt% organoclays, which were treated with different surfactants, at cooling rate 5°C/min.....	79
E.2 DSC cooling curves of EVOH/clay nanocomposite films containing 3 wt% organoclays, which were treated with different surfactants, at cooling rate 20°C/min.....	80
E.3 DSC cooling curves of EVOH/clay nanocomposite films containing different MMT_T organoclay loadings, at cooling rate 5°C/min.....	81
E.4 DSC cooling curves of EVOH/clay nanocomposite films containing different MMT_T organoclay loadings, at cooling rate 20°C/min.....	82

CHAPTER I

INTRODUCTION

1.1 General Introduction

Packaging has had important role in many industries. The packaging is used to contain, protect contamination and damages caused by physical force, moisture, oxygen and weather condition on object in the package. Polymers are the most regularly material used for packaging. Polymers can produce transparent packaging, reduce packaging weight, various process packaging shape and not broken like glass packaging. The polymers are used in packaging such as polyethylene (PE), high density polyethylene (HDPE), low density polyethylene (LDPE), linear low density polyethylene (LLDPE), polypropylene (PP), polyamide (PA or nylon), polystyrene (PS), polyvinyl chloride (PVC), polyvinylidene chloride (PVDC), polycarbonate (PC) and ethylene vinyl alcohol copolymer (EVOH). The polymers are chosen by properties of packaging such as EVOH and PVDC, which are an excellent gas barrier [1]. In packaging films, almost packaging research tried to improve gas barrier properties (such as oxygen gas) as one of the primary trends in flexible packaging. The oxygen barrier films can protect the object in the package by hindering the permeation of oxygen in order to maintain quality of goods from deterioration by oxygen in the environment [2]. Therefore, the oxygen barrier films increase shelf life of the packaged. Polymer/clay nanocomposites are one of choices for gas barrier films. The addition of a small amount of nanoclay filler (3-5 wt%), which properly dispersed in the polymer matrix and forms interaction with the polymer chains, can extremely enhance performance such as tensile strength, modulus, heat distortion temperature and gas barrier [3-4]. Moreover, producing polymer/clay nanocomposites is an cost effective way to enhance both mechanical and gas barrier properties of polymer by adding only 3-5 wt% of clay into polymer.

For this research, Ethylene vinyl alcohol copolymer (EVOH)/clay nanocomposite films were studied in order to apply for gas barrier films. EVOH copolymers and clays were polymer matrix and nanofiller, respectively. EVOH copolymers are highly crystalline and transparent polymer with very small free volume compared to other polymers such as Polyethylene (PE), Polypropylene (PP) and Polyamide (Nylon) [1,5]. Nanoclays, which consist of the silicate layers and obtain high surface area and high aspect ratio, are flat platelets [6]. The incorporation of EVOH copolymers and nanoclays created tortuous path of gases because the pathway of gases was hindered by silicate layers of clay dispersed in EVOH matrix [2]. Accordingly, EVOH/clay nanocomposites show excellent gas barrier properties. However, the properties of nanocomposites were very good when the clays were treated by suitable surfactant type and the nanocomposites were created by optimum organoclay loading. Consequently, the effect of surfactant and organoclay loading on mechanical and gas barrier properties of EVOH/clay nanocomposite film was studied for this research.

1.2 Objectives of the Present Study

1. To study the effect of surfactant structure on the degree of clay dispersion in organoclay and EVOH/clay nanocomposite film.
2. To investigate the effect of organoclay loading on the mechanical, thermal and gas barrier properties of EVOH/clay nanocomposite film.
3. To evaluate the relationship between the degree of clay dispersion and mechanical, thermal and gas barrier properties of EVOH nanocomposite film.

1.3 Scopes of the Present Study

1. Choose several kinds of surfactants to treat surface of clay.

- Octadecylmethyl[polyoxyethylene (15)] ammonium chloride
(Ethoquad 18/25)
- Cocoalkylmethyl[polyoxyethylene (15)] ammonium chloride
(Ethoquad C/25)
- Cocoalkylmethylbis(2-hydroxyethyl) ammonium chloride
(Ethoquad C/12-75)
- Oleylmethylbis(2-hydroxyethyl) ammonium chloride
(Ethoquad O/12 PG)
- Trimethyl tallow quaternary ammonium chloride
(Arquad T-50)
- Dimethyl bis(hydrogenated-tallow) ammonium chloride
(Arquad 2HT-75)

2. Investigate the optimum conditions to obtain EVOH/clay nanocomposite films, which contain 1%, 3%, 5% and 7% organoclay loading.

3. Study the effect of surfactants and organoclay loading on mechanical, thermal and barrier properties of EVOH/clay nanocomposite films.

สถาบันวิทยบริการ
จุฬาลงกรณ์มหาวิทยาลัย

CHAPTER II

THEORY

2.1 EVOH copolymers

Ethylene-vinyl alcohol (EVOH) copolymers are a family of random semicrystalline copolymer of ethylene and vinyl alcohol. They are commonly produced via a saponification reaction of a parent ethylene-co-vinyl acetate copolymer, whereby the acetoxy group is converted into a secondary alcohol [7-8]. A molecular structure of EVOH copolymers are shown below:

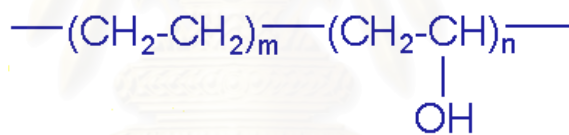


Figure 2.1 The structure of EVOH copolymers

EVOH copolymers are mostly used as material for food packaging industry because they are strong, flexible and transparent. They also obstruct the permeation of flavour, aroma, and gas such as oxygen, nitrogen, carbon dioxide and helium. Furthermore, the surface of EVOH copolymers could easily be printed without any particular treatment [7-9].

Table 2.1 The oxygen gas transmission rate of various grades of EVOH copolymers [8]

EVAL™ Resins Grade	Ethylene content mol%	O ₂ GTR at 20°C - 65%RH (cc.20μm/m ² .day.atm)
EVAL™ L	27	0.2
EVAL™ F	32	0.4
EVAL™ T	32	0.5
EVAL™ J	32	0.6
EVAL™ H	38	0.7
EVAL™ E	44	1.5
EVAL™ G	47	3.2

Note: EVAL™ resin is the registered trademark for the EVOH copolymer resins manufactured and marketed by Kuraray.

From table 2.1, the oxygen barrier properties of EVOH copolymers increase with decreasing the content of ethylene in molecular structure. EVOH copolymers with low contents of ethylene (<32 mol%) show outstanding barrier properties to gases compared to other polymers such as polyethylene, polypropylene and nylon (show as table 2.2) [7,9].

EVOH copolymers are excellent gas barrier because EVOH copolymers have been attributed to its smaller free volume than other polymers. But, EVOH copolymers show poor moisture resistance. As moisture content increases, crystalline structure of EVOH copolymers is plasticized and pathways for gas molecules are created. Therefore, the gas barrier properties of EVOH copolymers are deteriorated at high moisture content [1,5,7].

Table 2.2 Barrier properties Comparison of Various Polymers [10]

Material	OTR @ 25°C, 65% RH (cc.µm/m ² .day.atm)	MVTR @ 40°C, 90% RH (gram.µm/ m ² .day.atm)
EVOH	19.68~70.87	551.18~2,125.98
PVDC	59.06~354.33	39.37~78.74
Acrylonitrile	314.96	1,968.50
MXD6	59.06	1,259.84
Oriented PET	1,023.62	472.44
Oriented Nylon	826.77	3,543.30
LDPE	165,354	393.7~590.55
HDPE	59,055	157.48
Polypropylene	59,055	271.65
Polystyrene	137.795	2,755.90~3937

Note: OTR = Oxygen Transmission Rate, or permeation rate of oxygen through material

MVTR = Moisture Vapor Transmission Rate, or permeation rate of water vapor through material

2.2 Clay and Organoclay

2.2.1 Clays

Clays are naturally occurring minerals. Clays are a hydrous aluminium phyllosilicate (phyllosilicates are a subgroup of silicate minerals). Almost the polymer/clay nanocomposites used smectite-type clays (such as montmorillonite, hectorite and synthetic mica).

In this study, montmorillonite or bentonite (or bentone) is used to enhance properties of EVOH copolymers such as mechanical and barrier properties. The chemical formular of montmorillonite is $\text{Na}_2\text{CaAl}_2\text{Si}_4\text{O}_{10}(\text{OH})_2(\text{H}_2\text{O})_{10}$, which depends on clay origin, and has a 2:1 layer structure which is shown below:

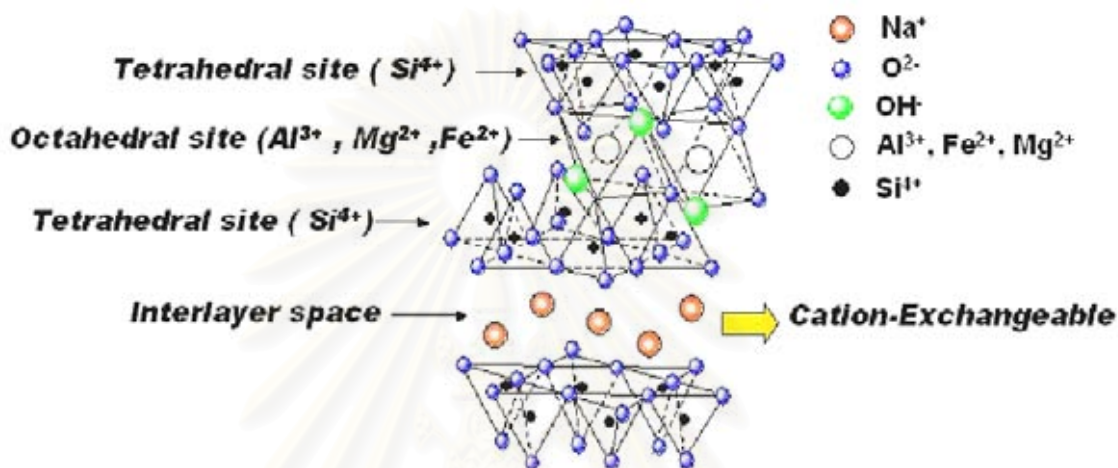


Figure 2.2 The crystal structure of montmorillonite or bentonite [11]

Figure 2.2 showed crystal lattice of montmorillonite that consists of an alumina octahedral (AlO_6) sheet sandwiched between two silica tetrahedral (SiO_4) sheets. The thickness of the layers is about 1 nm and its diameter is in the range of 100-1500 nm, hence its high aspect ratio has been observed. Therefore, clay platelets are truly nanoparticles when exfoliated [6]. In addition, the clays are generally highly hydrophilic.

2.2.2 Organoclay

The nature of original clay surfaces is highly hydrophilic. It impedes their homogeneous dispersion in the organic polymer phase. Clay is incompatible with polymer e.g. polyethylene, polypropylene, nylon and EVOH copolymers. Therefore, the surface treatment of clay is necessary in order to change property of clay surface from hydrophilic to hydrophobic (or organophilic). The one of alternative methods is ion exchange with organic cation (surfactant) such as a quaternary ammonium ion.

The treated clay is called modified clay, organophilic clay or organoclay as shown in figure 2.3 [12].

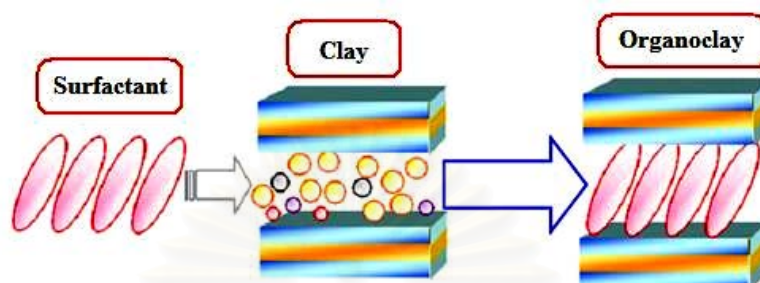
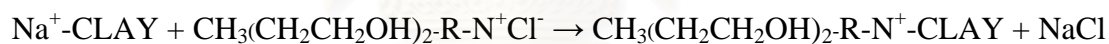


Figure 2.3 The treatment of clay by ion exchange with organic cation [13]

For example, the sodium ions in the montmorillonite could be exchanged for an ammonium ion such as Oleylmethylbis(2-hydroxyethyl) ammonium chloride (Ethoquad O/12 PG):



2.3 Polymer/Clay Nanocomposites

Polymer/clay nanocomposites are constructed by mixing nanoparticles (clay), whose form is flat platelets, with polymer matrix. These platelets are distributed into a polymer matrix creating multiple silicate layers which force gases to flow through the polymer matrix in a torturous path. The torturous path forms complex barriers to gases such as oxygen, nitrogen and carbon dioxide.

2.3.1 The Methods for Polymer/Clay Nanocomposite Preparation

Three methods are developed to produce polymer/clay nanocomposites, i.e. in situ polymerization, solution induced intercalation (solvent method) and melt processing (melt compounding). Clays are added directly to liquid monomer during

the polymerization state in in situ polymerization method. Clay are then expanded and dispersed into the matrix. This method is capable of producing well-exfoliate nanocomposites. Unlike in situ polymerization method, the clays are added to a polymer solution using solvents such as toluene, chloroform and acetonitrile to integrate the polymer and clay molecules in solution induced intercalation method. This method poses difficulties for the commercial production because of high cost of solvents required. Large amount of solvent is needed to achieve appreciable filler dispersion; therefore, health and safety problem are concerned. However, this method is applicable to water-soluble polymers, because of the low cost and low health and safety risks. Unlike other two methods mentioned above, melt processing method, the silicated layers are directly dispersed into polymers during its melting. The polymer pellets and clays are processed through an extrusion machine. They are pressed together using shear forces to help with exfoliation and dispersion of clay. This method is thus more suitable for commercial production of nanocomposites than the in situ polymerization method because the melt processing method, starting material is polymer pellets but in the in situ polymerization method it is started with liquid monomer, which is complicated [6].

2.3.2 The Formation of Polymer/Clay Nanocomposite

From three produced polymer/clay nanocomposites methods, the incorporation of polymer and clays have been classified into three major types depending on the dispersion of clays in the polymer matrix.

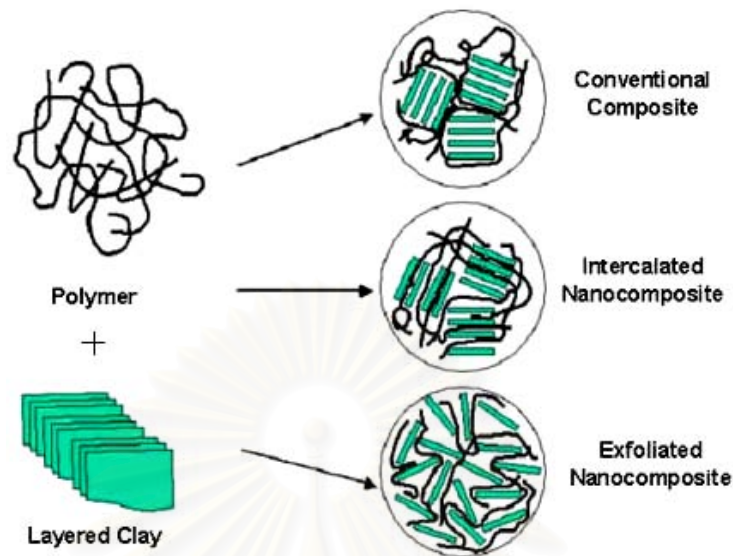


Figure 2.4 The formation of polymer/clay nanocomposite [14]

From figure 2.4, the first type is a conventional composite or microcomposite where the polymer chains could not insert through the silicate layer stacks. Second one is the intercalated nanocomposite where the polymer chains could insert through the silicate layer stacks. Therefore, the interlayer spacing of silicate layers is expanded but the order of the silicate layers is still maintained. The last one is exfoliated nanocomposites where the silicate layers are delaminated as an individual layer and distributed randomly in the polymer matrix [14].

2.4 EVOH/Clay Nanocomposites

In this study, gas barrier properties of polymer are prior considered because one of the important properties of packaging films is to control gas permeability and to obstruct the flow of gases passing films. Consequently, EVOH copolymers are the best choice, compare to other polymers such as polyethylene, polypropylene and nylon. Due to the free volume of EVOH copolymers, which is smaller than other polymers, EVOH copolymers films show excellent gas barrier. From its properties, the gas barrier properties of EVOH copolymers can be enhanced by filled clay because the pathway of gases is obstructed by silicate layers dispersed in EVOH

matrix. Moreover, the mechanical properties of EVOH copolymers are enhanced by organoclay such as Young's modulus and tensile strength.

2.5 Processing Techniques

2.5.1 Polymer extrusion [Polymer process engineering]

Extrusion is one of the most common processes of polymer industry for mixing, compounding, or reacting polymeric materials. It has been classified into two major types depending on the number of screw in extruder: single screw extrusion and twin screw extrusion. In this study, the twin screw extrusion was used to compound polymer resins and reinforcement fillers.

2.5.1.1 Twin screw extrusion

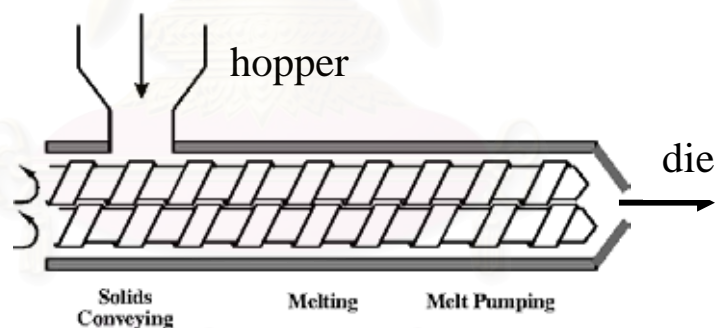


Figure 2.5 Schematic of a Twin screw extruder [15].

Figure 2.5 shows schematic of a twin screw extruder. In this process, the raw materials, which are composed of solid polymer resin and/or fillers, are fed into hopper. The polymers are melted and forced to flow through a die by the co-rotating screws in extrusion barrel. After that, the melted polymer is cooled by cooling bath and cut into polymer composite platelets.

2.5.1.2 Blown film Extrusion

Blown film extrusion is one of the film producing methods. From figure 2.6, polymer pellets are melted by twin-screw zone. Polymer melt was extruded through a blown film die (annular slit die) to form a thin walled tube. The tube of film then continues upwards until it passes through nip rolls. Air is introduced via a hole in the center of the die to blow up the tube like a balloon. Film width and thickness was controlled by controlling the volume of air in the bubble, the output rate of the extruder and the speed of the haul-off [16].

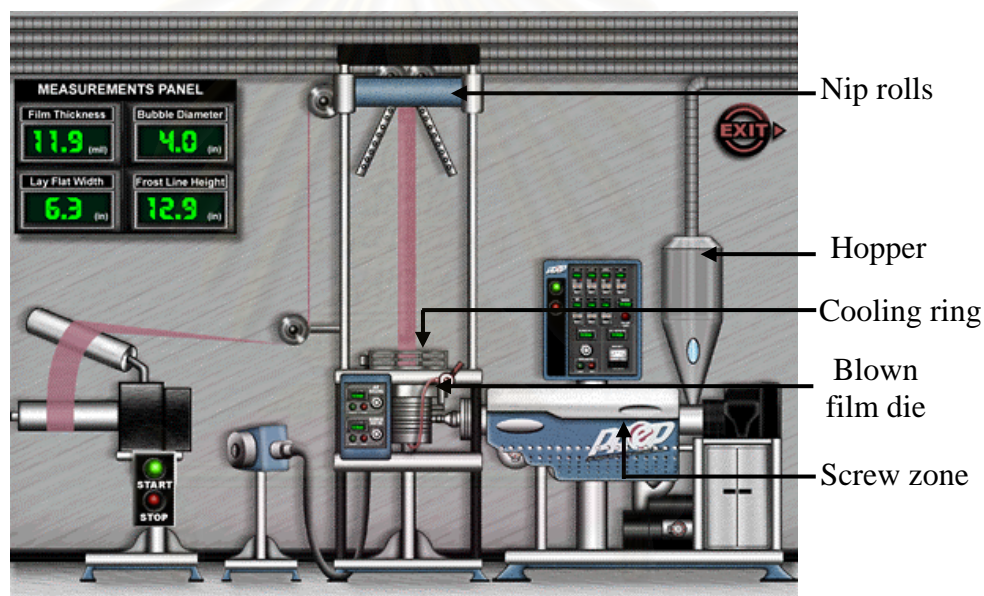


Figure 2.6 Diagram of a blown film extrusion line [17].

2.6 Characterizations

2.6.1 Mechanical Testing

Tensile properties indicate a behavior of material that reacts to forces being applied in tension. The results were obtained from measuring the applied load and the elongation of the specimen over some distance.

In this study, tensile properties of EVOH/clay nanocomposites were tested in accordance with ASTM D882 using an Universal testing machine (Instron 5567, USA) in order to determine the modulus, tensile strength and elongation at break shown as figure 2.7.

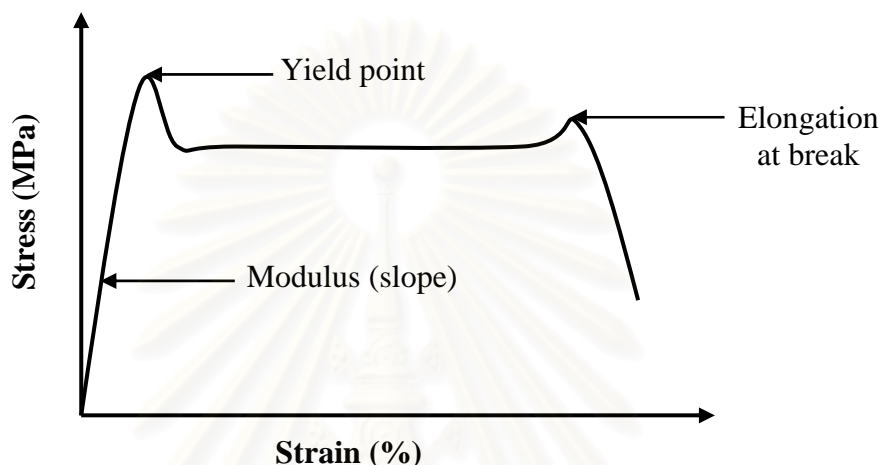


Figure 2.7 Diagram of stress/strain of sample under tension

In tension mode, the tensile modulus is the ratio of stress and strain. The ultimate elongation at break of engineering material obtains before it breaks. 100% ultimate elongation at break is common for film polyolefins. A high tensile modulus and high elongation at break mean that the material is rigid and tough [18].

2.6.2 X-ray Diffraction (XRD)

X-ray diffraction (XRD) is a technique used to determine the interlayer spacing of clay and organoclay, based on their characteristic diffraction behavior under X-ray irradiation of a known wavelength [19].

In this study, XRD patterns of EVOH/clay nanocomposites are obtained using D8 advance BRUKER German (figure 2.8) with $\text{CuK}\alpha$ radiation of wavelength 1.542 \AA at 40 kV and 30 mA at the ambient temperature.



Figure 2.8 X-ray diffractometer (D8 advance BRUKER German)

The results from XRD analysis have been classified into two major types depending on the pattern of graph shown as figure 2.9.

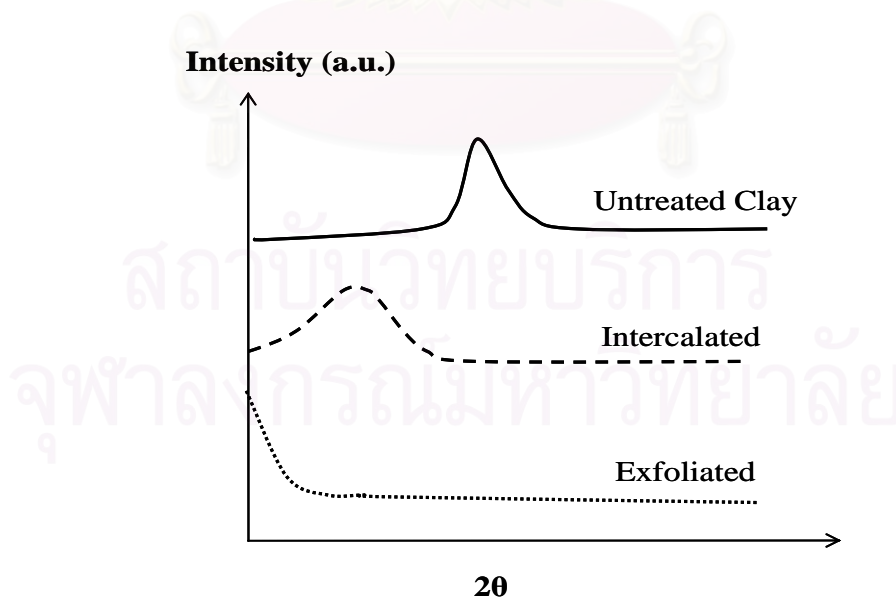


Figure 2.9 Diagram of X-ray diffraction analysis

From figure 2.9, the top line show diffraction curve of untreated clay. The organoclays, which is treated by ion exchange method with organic cation (surfactant) such as a quaternary ammonium ion, are mixed with polymer matrix in order to form nanocomposites. If the silicate layers of clay in polymer matrix are expanded but the order of the silicate layers is still maintained, the diffraction curve is shown as a middle line in figure 2.9. This curve shows peak, which is shifted to lower angle. If the silicate layers of clay in polymer matrix are delaminated as an individual layer and distributed randomly in the polymer matrix, the diffraction curve is shown as a bottom line in figure 2.9. There is no peak appeared in this curve.

The interlayer spacing of clay and organoclay (or degree of clay dispersion) is calculated by the Bragg's equation. Bragg's law is derived by physicists W.H. Bragg and his son. It was determined the spacing between the planes in the atomic lattice by the following equation:

$$n\lambda = 2d \sin \theta$$

- where
- n = Peaks correspond to the {001} basal reflection (n=1)
 - λ = The wavelength of the X-ray radiation used in the diffraction experiment (angstroms), which equals to 1.542 Å when CuK α was used.
 - d = The spacing between the planes in the atomic lattice (Å)
 - θ = The angle between the incident ray and the scattering planes (degrees)

2.6.3 Differential Scanning Calorimetry (DSC)

Differential scanning calorimetry (DSC) is a technique in which the amount of heat required to increase the temperature of a sample and reference, are measured as a function of temperature. As temperature increases, the sample, which is a partially crystalline polymer, is changed to amorphous form by adding energy to the sample making it be able to flow. Therefore, the crystalline-melting temperature (T_m) is an endothermic peak. As the temperature decreases, polymer chains try to arrange

themselves to be in an order form which is crystalline phase. Therefore, the crystallization temperature (T_c) is an exothermic peak in the DSC curve [20-21]

The crystallinity of the sample can be calculated from the area of the endothermic peak of the DSC curve, which is determined the melting enthalpy (ΔH_f) compared to 100% crystalline sample ($\Delta H_{f,100\%}$). The crystallinity of sample is given by the equation [21]:

$$a = \frac{\Delta H_f}{\Delta H_{f,100\%}} \times 100\%$$

where a = The percent of crystallinity of sample (%)

ΔH_f = The melting enthalpy of sample

$\Delta H_{f,100\%}$ = The melting enthalpy of 100% crystalline sample

2.6.4 Oxygen Transmission Rate (O_2TR)

Oxygen transmission rate (O_2TR) is the measurement of the amount of oxygen gas that passes through sample over a given period (diffusion mode). In this study, oxygen transmission rate (O_2TR) of EVOH/clay nanocomposites is determined by Oxygen gas transmission apparatus (figure 2.10) at 25°C and 65-68 % R.H., according to ASTM D3985.



Figure 2.10 Oxygen gas transmission apparatus

CHAPTER III

LITERATURE REVIEWS

The gas (such as oxygen gas) barrier property of film is important for film packaging industry because the oxygen barrier film can protect the object in the packaging, which obstructs the permeation of oxygen in environment, in order to maintain quality and increase shelf life of the packaged. Therefore, the improvement of the gas barrier property of film was studied as primary research of film packaging. The polymer/clay nanocomposites are the one of choice for this study. Because the small amount of nanoclays (3-5 wt%), which consist of silicate layers, contain high aspect ratio and high surface area, dispersed in the polymer matrix and formed interaction with polymer chains, the nanocomposites show better mechanical, thermal and gas barrier properties than pure polymer. Before the polymer is mixed with clays, the clays are treated by ion exchange method with organic cation (surfactant) such as a quaternary ammonium ion, which is called organoclay. The interlayer spacing of silicate layers of organoclay are increased by the treatment of clay. Fornes et al. (2002) [22] showed that the increase of spacing between the silicate layers (degree of clay dispersion) of several organoclay (molecular structure of three surfactants were used as shown in figure 3.1) had different scales, compare to pristine clay.

สถาบันวิทยบริการ
จุฬาลงกรณ์มหาวิทยาลัย

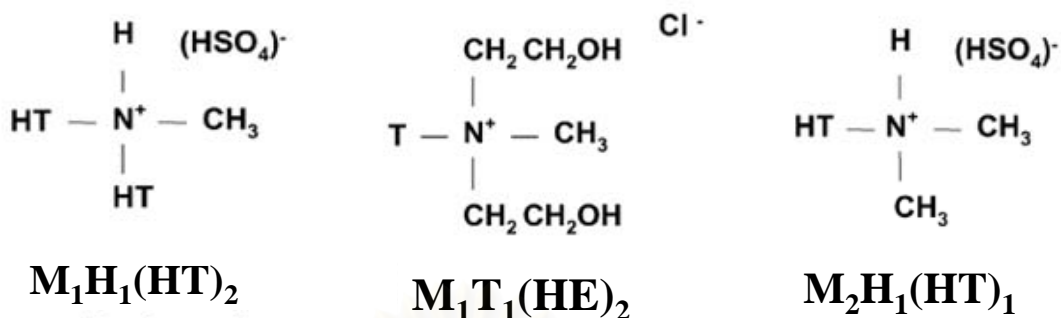


Figure 3.1 The molecular structure of three surfactants were used as examples:
 $M_1H_1(HT)_2$ is Methyl bis(hydrogenated-tallow) ammonium montmorillonite,
 $M_1T_1(HE)_2$ is Bis(2-hydroxy-ethyl)methyl tallow ammonium montmorillonite and
 $M_2H_1(HT)_1$ is Dimethyl hydrogenated-tallow ammonium montmorillonite [22]

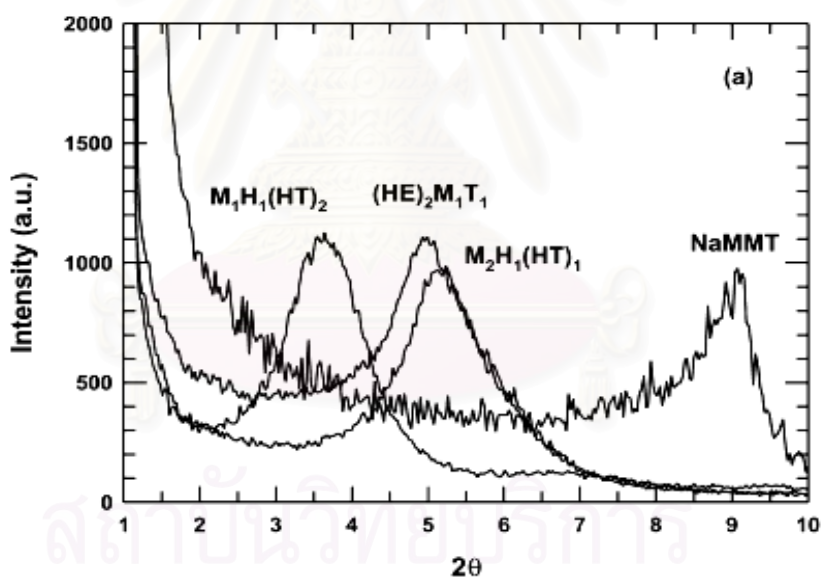


Figure 3.2 WAXS results for $M_1H_1(HT)_2$, $M_1T_1(HE)_2$ and $M_2H_1(HT)_1$ organoclays and pristine clay (NaMMT) [22]

From figure 3.2, the degree of clay dispersion of $M_1H_1(HT)_2$, $M_1T_1(HE)_2$ and $M_2H_1(HT)_1$ organoclays were observed at lower 2θ angles than that of pristine clay (NaMMT). Therefore, the three organoclays showed higher interlayer spacing of the silicate layers than pristine clay, calculated the Bragg's law. Ke and Yongping (2005)

[23] also reported that the interlayer spacing of silicate layers (d-spacing) of clay was increased by organically modified processing. The clays were treated by quaternary ammonium salt, which contained Cl^- and $-\text{COOH}$ in its structure. The d-spacing of organoclays were increased from 1.90 nm to 2.74 nm (increased 44%).

The clays, which were treated by ion exchange method, were mixed with polymer in order to form nanocomposite. The dispersion of silicate layers of clay in polymer matrix was important for improving mechanical, thermal and gas barrier properties of polymer/clay nanocomposites. The d-spacing of clay increased with mixing polymer. Frounchi e al. (2006) [24] reported that the d-spacing of clay increased with mixing PP/EPDM blend and increasing organoclay loading but no change in d-spacing when the mixing PP/EPDM blend with 7 wt% organoclay as shown in figure 3.3.

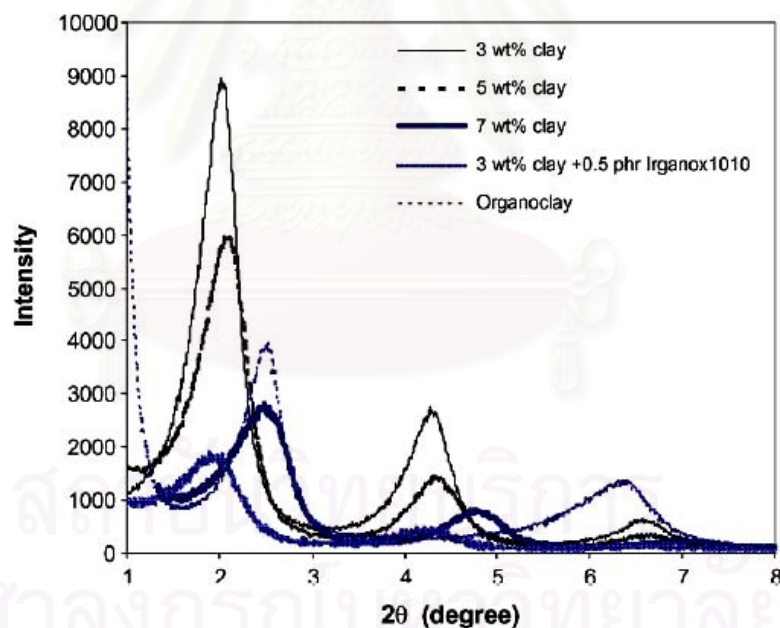


Figure 3.3 XRD curves of organoclay and PP/EPDM nanocomposites at various clay loading (3, 5 and 7 wt%) and 3 wt% with 0.5 phr compatibilizer [24].

The properties (such as mechanical, thermal and gas barrier) of polymer were improved by the incorporation of polymer and nanoclays. The improvement of mechanical properties of nanocomposites, such as tensile strength and modulus, was caused by the strength of silicate layers in nanoclay. Lin et al. (2003) [25] reported that the tensile modulus and yield strength of polyamide 6/layered silicate nanocomposites were increased with increasing organoclay loading as shown in figure 3.4 and 3.5.

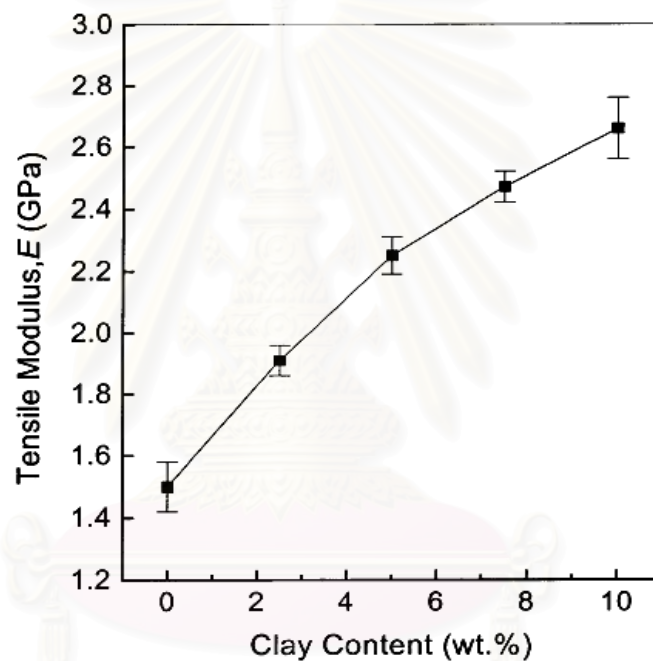


Figure 3.4 Tensile modulus of polyamide 6/clay nanocomposites at different clay loading (wt%) [25].

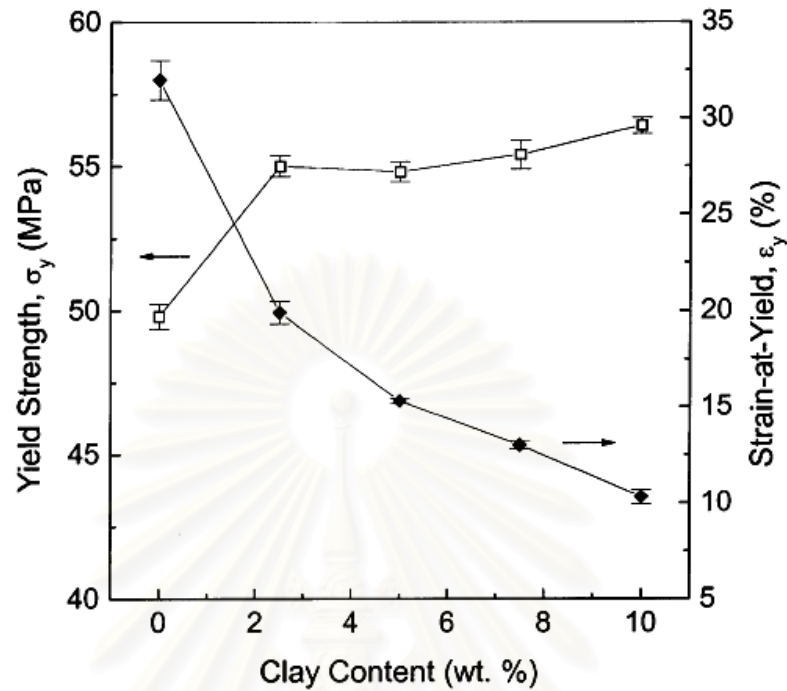


Figure 3.5 Yield strength and strain at yield of polyamide 6/clay nanocomposites at different clay loading (wt%) [25].

Thermal properties (the crystalline-melting temperatures and the crystallization temperatures: T_m and T_c , respectively) either increased or decreased with mixing polymer depended on surfactant type. Frounchi et al. (2006) [24] showed the melting temperature slightly decreased, when compounding PP/EPDM blend with organoclay. The percent of crystallinity, which was determined by heat of melting of PP/EPDM blend nanocomposites, also decreased, as shown in figure 3.6.

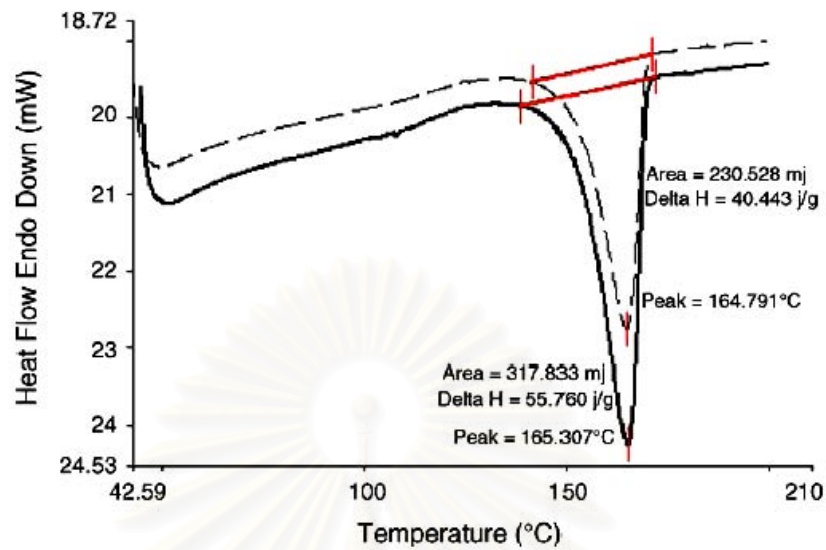


Figure 3.6 DSC heating curve for PP/EPDM blend without nanoclay (solid line) and with 3 wt% clay (dashed line) [24].

Furthermore, Ratna et al. (2006) [26] reported that the melting temperatures and the percent of crystallinity, which was determined by heat of melting of poly(ethylene oxide)/clay nanocomposites, were decreased with increasing organoclay loading, as shown in figure 3.7.

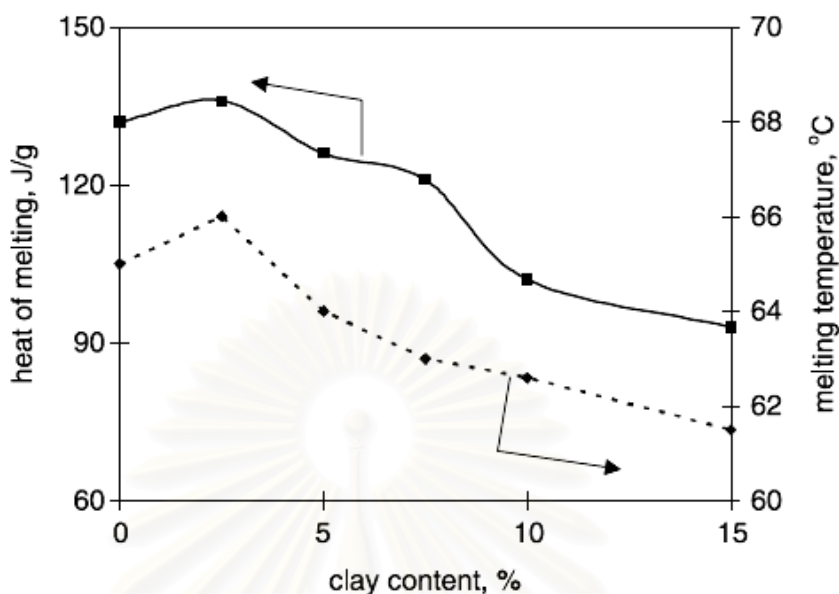


Figure 3.7 Melting temperature and heat of melting of poly(ethylene oxide)/clay nanocomposites at various organoclay loading [26].

In addition, the dispersion of silicate layers of clay in polymer matrix improved the gas barrier property of pure polymer. Frounchi et al. (2006) [24] showed the decrease of oxygen permeability of PP/EPDM blend nanocomposites. The gas barrier property of nanocomposites increased with increasing organoclay loading (increased 45% and 57% when mixing with 3 and 5 wt% organoclay, respectively) and decreased when mixing with 7 wt% organoclay but it was higher than pure PP/EPDM blend without organoclay (increased 33%).

Ethylene vinyl alcohol (EVOH) copolymer was an excellent gas barrier polymer because its free volumes were smaller than those of other polymers, such as PE, PP and nylon. Therefore, EVOH copolymer was one of choice for barrier packaging film. The obstruction of free volumes with silicate layers of clay was the best choice. The EVOH/clay nanocomposites were higher properties than pure EVOH such as mechanical, thermal and gas barrier properties. From previous researches, surfactant types affected the degree of clay dispersion of organoclay, which was mixed with EVOH copolymers [27-28]. In 2001 [27], Artzi et al. showed that the increase in interlayer spacing between the planes in the atomic lattice of organoclay,

which was treated by octadecylamine, from 2.46 nm, prior mixed with polymer, to 3.25 nm after mixed with EVOH copolymers. In 2002 [28], polyoxyethylene decyloxypropylamine was used to treat clay. The degree of clay dispersion of organoclay increases from 2.9 nm, prior mixed with polymer, to 3.2 nm after mixed with EVOH copolymers. Furthermore, they found that organoclay loading also affected the degree of clay dispersion. It increased from 3.25 to 3.6 nm with decreasing organoclay loading from 15 to 5 wt%. Due to the presence of the silicate layers of clay, which were dispersed in EVOH, the EVOH/clay nanocomposites exhibited higher modulus than pure EVOH copolymers. Froio et al. (2004) [29] found that Young's modulus decreased with increasing relative humidity. However, the EVOH/clay nanocomposites showed higher Young's modulus than pure EVOH as shown in figure 3.8. Therefore, the modulus of EVOH/clay nanocomposites was increased by the presence of silicate layers of clay.

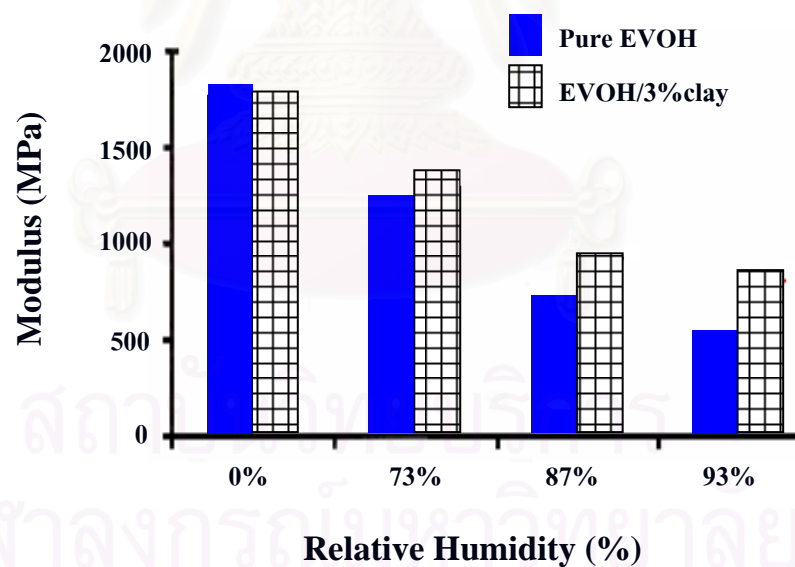


Figure 3.8 Modulus of EVOH/clay nanocomposites, which consisted of 3 wt% clay, at various percent of relative humidity [29].

CHAPTER IV

EXPERIMENTS

4.1 Materials

EVOH copolymer (Ethylene vinyl alcohol copolymer) used in this study is a commercial product (EVAL® E-105B), containing 44 mol% ethylene from Kuraray, Japan.

Na-Bentonite was supplied by Kunimine Industrial Co.,Ltd., Japan. It is untreated clay and has cation exchange capacity (CEC) of 90 meq/100g clay, according to ASTM C837-99.

In this study, six surfactants were used. Octadecylmethyl[polyoxyethylene (15)] ammonium chloride (Ethoquad 18/25), Cocoalkylmethyl[polyoxyethylene (15)] ammonium chloride (Ethoquad C/25), Cocoalkylmethylbis(2-hydroxyethyl) ammonium chloride (Ethoquad C/12-75), Oleylmethylbis(2-hydroxyethyl) ammonium chloride (Ethoquad O/12 PG), Trimethyl tallow quaternary ammonium chloride (Arquad T-50) and Dimethyl bis(hydrogenated-tallow) ammonium chloride (Arquad 2HT-75) were supplied by Akzo Nobel, Arnhem.

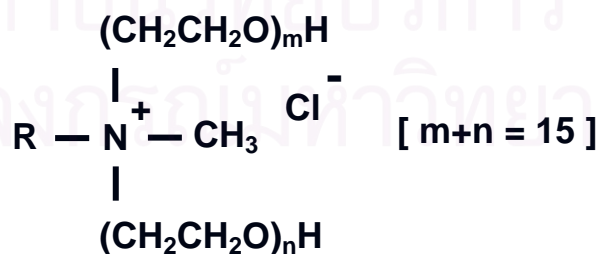


Figure 4.1 Octadecylmethyl[polyoxyethylene (15)] ammonium chloride (Ethoquad 18/25) [30]

From figure 4.1, the letter R represents alkyl chain which consists predominantly of chain with 18 carbons (~ 96.60%).

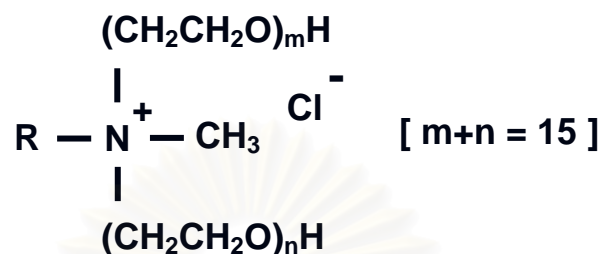


Figure 4.2 Cocoalkylmethyl[polyoxyethylene (15)]ammonium chloride
(Ethoquad C/25) [30]

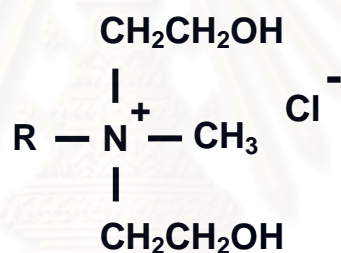


Figure 4.3 Cocoalkylmethylbis(2-hydroxyethyl)ammonium chloride
(Ethoquad C/12-75) [30]

From figure 4.2 and 4.3, the letter R denotes the product made from coconut oil which consists predominantly of chain with 12 carbons (~ 54%).

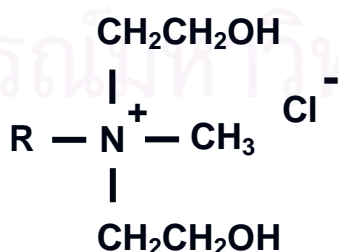


Figure 4.4 Oleylmethylbis(2-hydroxyethyl)ammonium chloride
(Ethoquad O/12 PG) [30]

From figure 4.4, the letter R denotes the product made from oleic acid which consists of chain with 18 carbons.

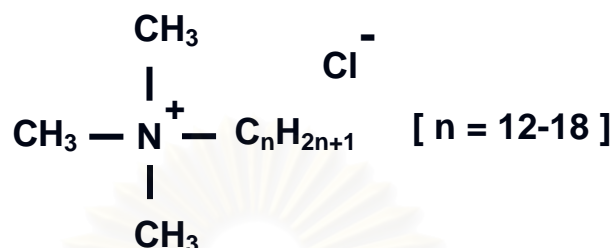


Figure 4.5 Trimethyl tallow quaternary ammonium chloride (Arquad T-50) [30]

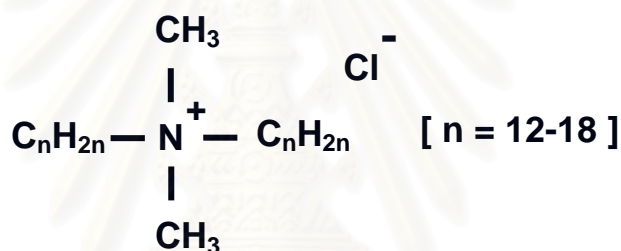


Figure 4.6 Dimethyl bis(hydrogenated-tallow) ammonium chloride
(Arquad 2HT-75) [30]

4.2 Preparation of the organoclay

Surface of Na-Bentonite were modified with ammonium salts by ion exchange process. The organoclay was formed by first dispersing Na-Bentonite in water, followed by the addition of the surfactant, which was dissolved in water at 70°C. The quantity of Ethoquad C/12-75, Ethoquad O/12PG, Ethoquad C/25 and Ethoquad 18/25 surfactants, were used in ion exchange process, was equal to CEC of clay. Arquad T-50 and Arquad 2HT-75 surfactants were used as 1.5 CEC of clay. The weight of surfactant was as follows:

$$g_{surf.} = \frac{CEC \times conc. \times Mw \times kg_{clay}}{\% assay}$$

Where $g_{surf.}$ = Weight of surfactant ($g_{surf.}$)
 CEC = Cation exchange capacity of untreated clay (meq/ g_{clay})
 conc. = Concentration of surfactant (mmol $_{surf.}$)
 Mw = Molecular weight of surfactant ($g_{surf.}/mol_{surf.}$)
 kg_{clay} = Weight of untreated clay (kg_{clay})
 % assay = Effectiveness of surfactant

After that, the solution was stirred continuously for 1 h. The product was then filtrated and washed by distilled water several times. The solid part was dried in an oven at 80°C until dried. After that it was ground into powder and sieved.

4.3 Preparation of EVOH/clay nanocomposites by melt processing

Before mixing, the EVOH copolymers and organoclay powders were dried in a vacuum oven at 105°C for 4 h. The components, which were dry-blended at 3% organoclay loading, were melt-mixed by twin screw extruder attached to blow film set (Thermo Haake Rheomex, Germany). Screw speed was 140 rpm and processing temperatures in zones 1-3 were 170, 195 and 195°C, respectively, and die was set at 200°C. Moreover, the components, which consisted of EVOH copolymers, clay and Arquad T-50 surfactant, were dry-blended at selected ratios (1%, 3%, 5% and 7% organoclay loading).

4.4 Characterizations

4.4.1 X-ray Diffraction (XRD)

X-ray diffraction (XRD) is a technique used to determine the interlayer spacing of clay and organoclay, based on their characteristic diffraction behavior under X-ray irradiation of a known wavelength [19].

In this study, XRD patterns were obtained using D8 advance diffractometer (BRUKER, German) with $\text{CuK}\alpha$ radiation of wavelength 1.542 \AA at 40 kV and 30 mA at the ambient temperature.

The interlayer spacing of clay and organoclay (or degree of clay dispersion) was calculated by the Bragg's equation

4.4.2 Mechanical Testing

Mechanical testing of EVOH/clay nanocomposites were carried out at room temperature in a Universal testing machine (Instron 5567, USA). In this study, the samples were tested only in machine direction (MD) shown as figure 4.7.

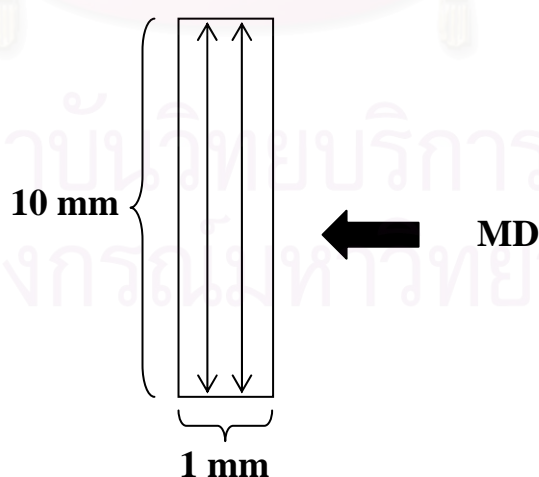


Figure 4.7 Tensile test sample.

A fixed crosshead rate of 50 mm/min was used in all cases and the results were taken as the average of ten tests. Rectangular shaped specimens were used according to the standard ASTM D882.

4.4.3 Differential Scanning Calorimetry (DSC)

Differential Scanning Calorimetry (DSC) is a technique used to determine the melting temperature (T_m) and crystallization temperature (T_c) [20]. In this study, it consisted of a heating scan from 45°C to 180°C at 10°C/min, followed by an isothermal at 180°C for 3 min and a subsequent cooling scan to 45°C at selected rate (5, 10 and 20°C/min). Melting and crystallization temperature were determined from heating and cooling step, respectively.

4.4.4 Oxygen Transmission Rate (O_2TR)

In this study, oxygen transmission rate (O_2TR) of EVOH/clay nanocomposite films is determined by MOCON OX-TRAN® 2/21. The samples were rectangular shape and tested at 23°C, 0 %R.H and 1 atm, according to ASTM D3985.

CHAPTER V

RESULTS AND DISCUSSION

EVOH/clay nanocomposite films were prepared by twin-screw extruder attached to blow film set at screw speed 140 rpm and processing temperatures in zones 1-3 were 170, 195 and 195°C, respectively, and die was set at 200°C. In this study, the effect of surfactant and organoclay loading on mechanical, thermal and gas barrier properties of EVOH/clay nanocomposite film was studied.

In this study, the MMT_C12/2 and EVOH_C12/2 represented the organoclay and EVOH/clay nanocomposite, respectively, which were compounded with Ethoquad C/12-75. The word C12/2 represented surfactant predominantly consisted of one alkyl chain with 12 carbons and 2 repeating units of oxyethylene. The rest organoclays and nanocomposites were referred in the same way. The MMT_T and MMT_2HT represented the organoclays, which were compounded with Arquad T-50 and Arquad 2HT-75, respectively. The letter T and term HT denoted surfactants, which consisted of tallow, predominantly chains with 18 carbons, and hydrogenated tallow, respectively.

5.1 Effect of surfactant types on EVOH/clay nanocomposite films' properties.

The surfactant types, which treated clays to modify their surface, were studied because the structure of surfactant and the reaction between polymer and surfactant, which was changed ion with clay, affected the mechanical, thermal and gas barrier properties of EVOH/clay nanocomposite films. The number of carbon atoms in alkyl chain and the number of oxyethylene groups of surfactant structures had an influence on clay dispersion in EVOH matrix and nanocomposite films' properties. In this study, six surfactants were divided into 3 groups:

1. The short (C12) and long (C18) alkyl tail surfactant groups:
 - C12/2 (represented Ethoquad C/12-75) and C18/2 (Ethoquad O/12PG), respectively.
 - C12/15 (Ethoquad C/25) and C18/15 (Ethoquad 18/25), respectively.
2. The one and two alkyl tail surfactant groups:
 - T (Arquad T-50) and 2HT (Arquad 2HT-75), respectively.
3. The number of repeating units of oxyethylene:
 - C12/2 (Ethoquad C/12-75), 2 units, and C18/15 (Ethoquad C/25), 15 units.

The EVOH/clay nanocomposites, which were prepared with different organoclays (C12/2, C18/2, C12/15, C18/15, T and 2HT) by melt processing using twin-screw extruder attached to blown film die, containing 3 wt% organoclay were used in this study.

5.1.1 Degree of clay dispersion of EVOH/clay nanocomposite films

The interlayer spacing of organoclays and the degree of clay dispersion of EVOH/clay nanocomposites were determined by the calculation from the 2θ position of the first diffraction (001) peak, which was determined by X-ray diffraction, using Bragg's law.

Figure 5.1 showed the X-ray diffraction patterns of pristine clay and organoclays, which were treated by different surfactant. The pristine clay showed diffraction (001) peak at $2\theta = 7.15^\circ$, corresponding to an interlayer spacing of clay of 1.23 nm. When pristine clay was treated by ion exchange method with quaternary ammonium ion surfactants, the diffraction (001) peak of organoclays had shifted to lower angles, compared to that of pristine clay. This new peak showed the larger interlayer spacing of clay, because the surfactants had inserted into the interlayer of silicate layers of clay [23-24,31-32].

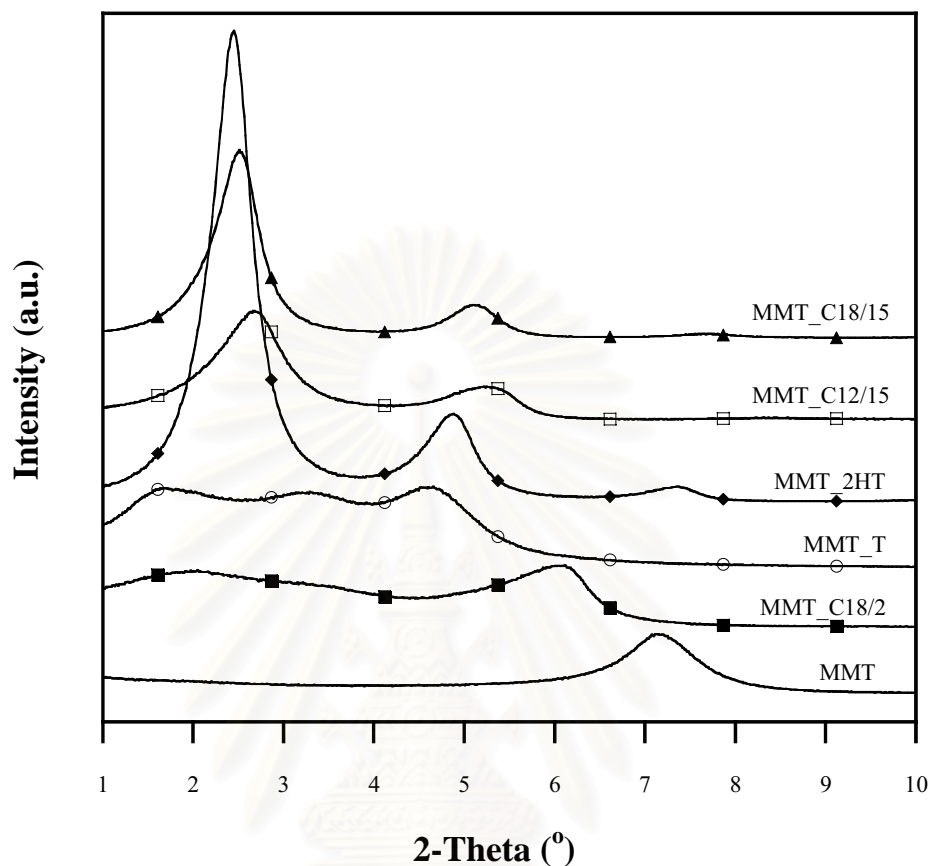


Figure 5.1 X-ray diffraction patterns of pristine clay and organoclays, which were treated by different surfactant: C18/2, T, 2HT, C12/15 and C18/15, at $2\theta = 1-10^\circ$.

When the organoclays were melt mixed with EVOH copolymers by twin-screw extruder attached to blown film set, they formed EVOH/clay nanocomposite films. The X-ray diffraction patterns of EVOH/clay nanocomposite films containing 3 wt% organoclays, which were treated with different surfactant types, at $2\theta = 1-10^\circ$ was shown in figure 5.2. The EVOH/clay nanocomposite films containing 3 wt% MMT_C12/2 organoclays showed the XRD curve was nearly flat, only small 3 peaks was observed at $2\theta = 2.00, 2.54$ and 2.94° , corresponding to an interlayer spacing of clay of 4.42, 3.47 and 3.00 nm, respectively. It indicated the larger interlayer spacing of clay in the nanocomposite film containing low molecular weight surfactant. In order word, organoclay was nearly exfoliated in nanocomposite film.

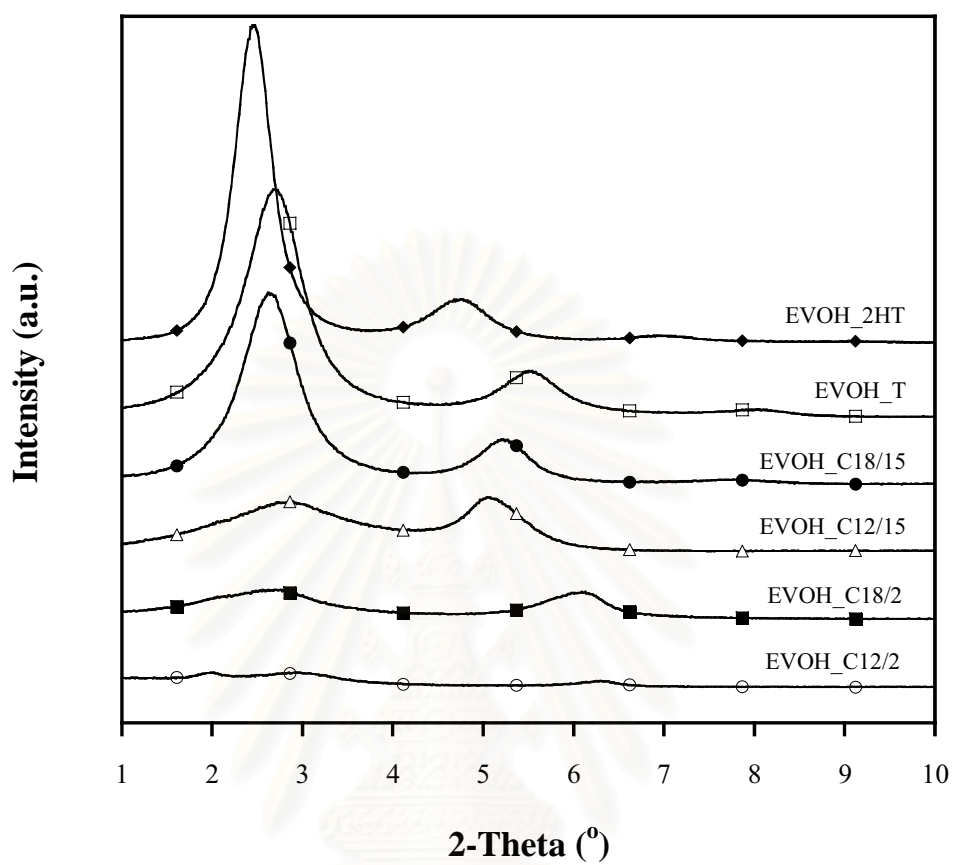


Figure 5.2 X-ray diffraction patterns of EVOH/clay nanocomposite films containing 3 wt% organoclays, which were treated with different surfactant types at $2\theta = 1-10^\circ$

สถาบันวิทยบริการ
จุฬาลงกรณ์มหาวิทยาลัย

5.1.1.1 Effect of the short (C12) and long (C18) alkyl tail surfactant

Figure 5.3 showed the X-ray diffraction patterns of organoclays and EVOH/clay nanocomposite films containing 3 wt% organoclays, which were treated by short (C12) and long (C18) alkyl chain surfactants: C12/15 and C18/15, respectively, at $2\theta = 1-10^\circ$. The MMT_C12/15 and MMT_C18/15 organoclays showed diffraction peaks at $2\theta = 2.68^\circ$ (3.29 nm) and 2.52° (3.51 nm), respectively.

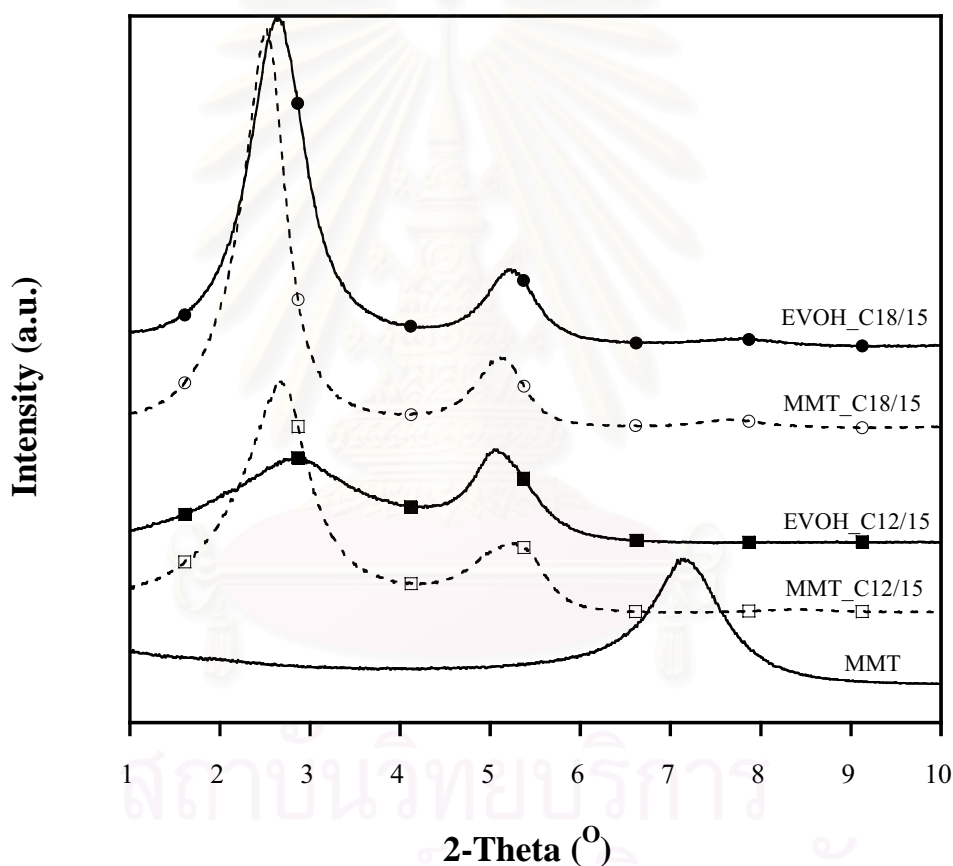


Figure 5.3 X-ray diffraction patterns of organoclays and EVOH/clay nanocomposite films containing 3 wt% MMT_C12/15 and MMT_C18/15 organoclays, at $2\theta = 1-10^\circ$.

After mixing EVOH copolymer with MMT_C12/15 and MMT_C18/15 organoclays, the nanocomposite films showed broader peak at slightly higher angle when compared to that of organoclays. They were observed at $2\theta = 2.87$ and 2.64° ,

respectively, corresponding to an interlayer spacing of 3.08 and 3.34 nm, respectively. The decrease in interlayer spacing of silicate layers in EVOH_C12/15 and EVOH_C18/15 nanocomposite films indicated that the surfactants were rearranged between silicate layers when mixing EVOH copolymer with organoclays. However, the order of silicate layers in EVOH_C12/15 and EVOH_C18/15 nanocomposite films was less than that of organoclays, which was signified by the broadening of peak. Moreover, the EVOH_C12/15 nanocomposite film exhibited broader peak than EVOH_C18/15 nanocomposite films. Therefore, the silicate layers of clay in nanocomposite films containing short (C12) alkyl chain surfactant were more disorder than those treated by long (C18) alkyl chain surfactant. In addition, EVOH_C12/15 and EVOH_C18/15 nanocomposite film exhibited intercalated-exfoliated nanocomposite and intercalated nanocomposite, respectively, compared to that of organoclays. Furthermore, the XRD pattern of EVOH_C12/15 nanocomposite film exhibited two peaks at $2\theta = 2.87$ and 5.07° , corresponding to an interlayer spacing of 3.08 and 1.74 nm, respectively. This result could be due to the variation of surfactant's chain orientation in interlayer spacing between silicate layers of clay [33].

5.1.1.2 Effect of the number of repeating units of oxyethylene

Figure 5.4 showed the X-ray diffraction patterns of EVOH/clay nanocomposite films containing 3 wt% organoclays, which were treated by surfactants containing 2 and 15 repeating units of oxyethylene: C12/2 and C12/15, respectively. The EVOH_C12/2 nanocomposite film showed lower 2θ and broader peak than EVOH_C12/15 nanocomposite film, indicating that the dispersion of clay in EVOH_C12/2 nanocomposite films were higher than that of EVOH_C12/15 nanocomposite film. This result could be due to the molecular size of surfactant.

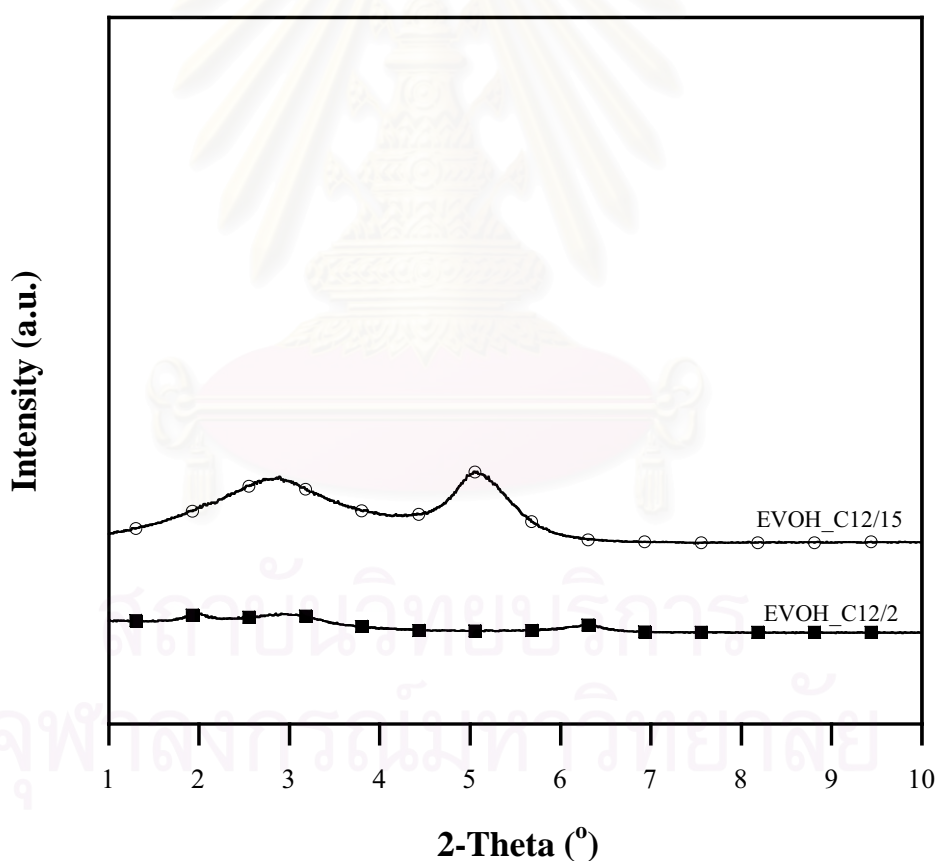


Figure 5.4 X-ray diffraction patterns of EVOH/clay nanocomposite films containing 3 wt% MMT_C12/2 and MMT_C12/15 organoclays

5.1.1.3 Effect of the number of alkyl tail surfactant

Figure 5.5 showed the X-ray diffraction patterns of organoclays and EVOH/clay nanocomposite films, which were treated by surfactants containing one alkyl tail and two alkyl tail surfactants. The MMT_T organoclay showed three diffraction (001) peaks, 1.67, 3.31 and 4.65°, corresponding to interlayer spacing of 5.27, 2.67 and 1.90 nm, respectively. This result was caused by the orientation of surfactant in interlayer spacing of clay. When the MMT_T organoclay were melt mixed with EVOH copolymers, showing peak at $2\theta = 2.7^\circ$ (3.27 nm), the dispersion of clay in EVOH matrix was more uniform than that of MMT. The MMT_2HT organoclay gave first peak at $2\theta = 2.45^\circ$, corresponding to interlayer spacing of 3.60 nm. The higher order MMT_2HT's diffraction peak indicated the clay stacking. When the MMT_2HT organoclay were melt mixed with EVOH copolymers, the nanocomposite film showed peak at $2\theta = 2.46^\circ$ (3.59 nm), which was the same peak as MMT_2HT's peak. This result meant that the EVOH chains did not intercalate into the interlayer spacing of the clay. Therefore, EVOH_2HT nanocomposite film was conventional composite. However, the diffraction peak of EVOH_2HT nanocomposite film was broader than that of organoclay, indicating the disorder structure of silicate layers of clay in nanocomposite film.

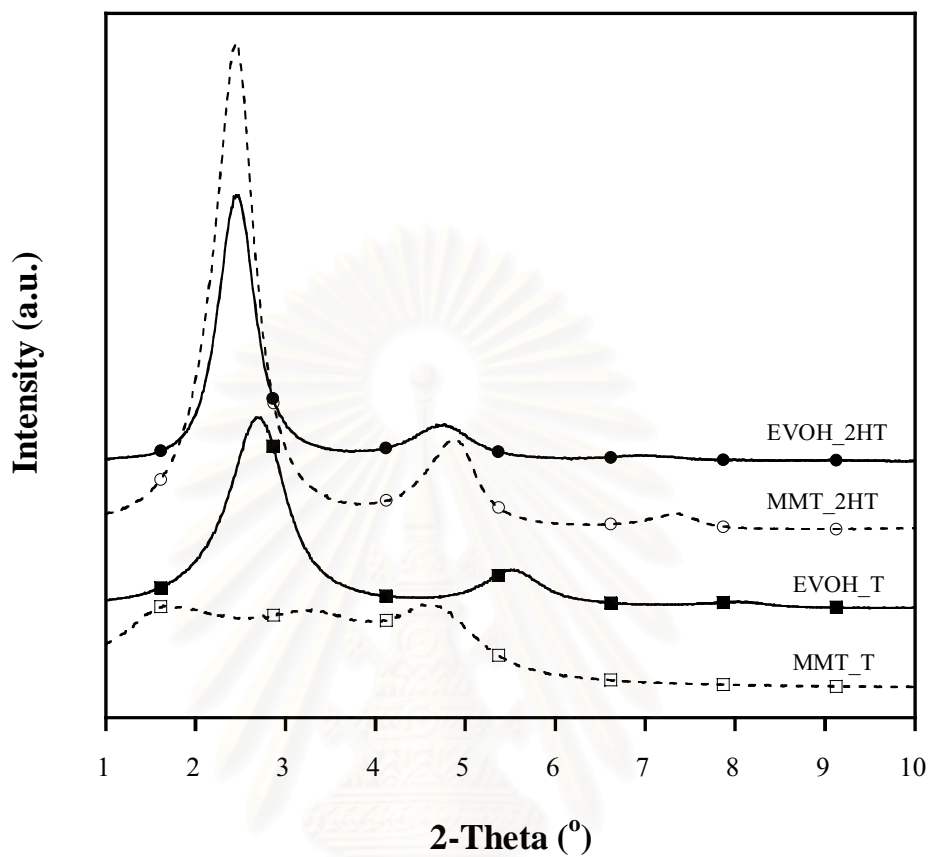


Figure 5.5 X-ray diffraction patterns of organoclays and EVOH/clay nanocomposite films containing 3 wt% MMT_T and MMT_2HT organoclays

Moreover, the EVOH/clay nanocomposite films containing one alkyl tail surfactant showed broader dispersion of clay than those treated by two alkyl tail surfactant, confirmed by the broader peak of EVOH_T nanocomposite film.

5.1.1.4 Degree of crystallinity of EVOH/clay nanocomposite films

The degree of crystallinity of EVOH/clay nanocomposite films was determined by the area under XRD peak at $2\theta = 19-22^\circ$ as shown in figure 5.6. The diffraction peak of all nanocomposite films were observed around $2\theta = 20.3-20.5^\circ$, corresponding to orthorhombic crystal structure of polymer, the same as that of the pure EVOH [34]. Therefore, they were no change of crystalline lattice when mixing EVOH copolymer with organoclays. Moreover, the area under diffraction peak of the films (EVOH_C18/2, EVOH_T and EVOH_2HT) increased when mixing EVOH copolymer with organoclays, compared to that of pure EVOH. However, the EVOH_18/15 films containing long (C18) alkyl chain and 15 repeating units of oxyethylene surfactant showed slightly smaller area under peak than pure EVOH film. The area under XRD's peak indicated the degree of crystallinity of nanocomposite film. Therefore, the degree of crystallinity of EVOH/clay nanocomposite films depended on surfactant types. The degree of crystallinity of nanocomposite film increased when treated with MMT_C18/2, MMT_T and MMT_2HT except nanocomposite films containing short (C12) alkyl chain surfactant whose degree of crystallinity decreased by half. Consequently, the short (C12) alkyl chain surfactants hindered crystallization process of EVOH/clay nanocomposite films. The increase of degree of crystallinity of nanocomposite films indicated that the organoclay, which was treated by long (C18) alkyl chain surfactant, behaved as nucleating agent.

From figure 5.6, the degree of crystallinity of EVOH_C18/2 and EVOH_C18/15 nanocomposite films were 100% and 45% higher than EVOH_C12/2 and EVOH_C12/15 films, respectively. Therefore, the nanocomposite films containing long (C18) alkyl chain surfactant showed higher degree of crystallinity than those treated by short (C12) alkyl chain surfactant. In addition, the nanocomposite films containing one alkyl tail surfactant showed 59 percent higher degree of crystallinity than those treated by two alkyl tail surfactant. This result could be due to the order of silicate layers of clay. The higher order of silicate layers of clay in nanocomposite films corresponded to higher degree of crystallinity of nanocomposite films

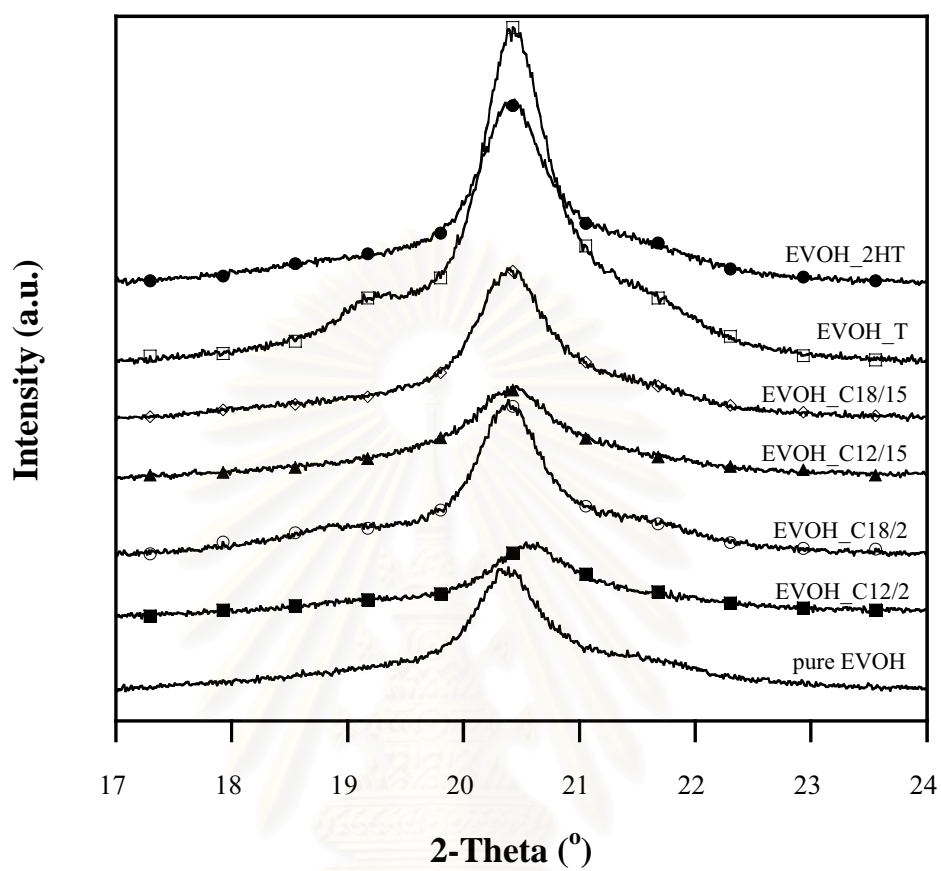


Figure 5.6 X-ray diffraction patterns of EVOH/clay nanocomposite films containing 3 wt% organoclays, which were treated with different surfactant types at $2\theta = 17\text{-}24^\circ$.

สถาบันวิทยบริการ
จุฬาลงกรณ์มหาวิทยาลัย

5.1.2 Thermal properties of EVOH/clay nanocomposite films

The thermal properties of EVOH/clay nanocomposite films, such as the crystalline-melting temperature (T_m) and the crystallization temperature (T_c), were determined by Differential scanning calorimetry (DSC). The crystalline-melting temperature (T_m) and the crystallization temperature (T_c) was an endothermic peak and an exothermic peak in the DSC curves, respectively.

Figure 5.7 showed the DSC melting curves of EVOH/clay nanocomposite films containing 3 wt% organoclays, which were treated with different surfactant types, at heating rate of 10°C/min. The crystalline-melting temperatures (T_m) were slightly changed, which were caused by surfactant types. They had low standard deviation with the value of 0.4°C. Consequently, the adding of organoclays, which were treated by different surfactant, in EVOH copolymer did not significantly affect the crystalline-melting temperatures of EVOH/clay nanocomposite films. Moreover, the degree of crystallinity of EVOH/clay nanocomposite films was determined by the area under DSC melting curve. The area under melting peak of nanocomposite films decreased compared to pure EVOH, indicating the decrease in degree of crystallinity of EVOH/clay nanocomposite films. Therefore, the clays affected the spherulite structure of EVOH copolymer and hindered the crystallization process [23-24,27]. This result was not consistent with the one calculating by the area under the diffraction peak of XRD technique. Because the EVOH/clay nanocomposite films were melted crystalline part of EVOH copolymer in order to obtain the crystalline-melting temperatures (T_m) of nanocomposite films in DSC technique. The EVOH chain could be rearranged and formed other crystalline phase again before completely melted. However, the XRD technique directly analyzed the crystalline phase of nanocomposite films without preheating. Therefore, the degree of crystallinity of EVOH/clay nanocomposite films, which was determined by DSC technique, could not be consistent with XRD technique.

The DSC cooling curves of EVOH/clay nanocomposite films containing 3 wt% organoclays, which were treated with different surfactant types, at cooling rate of 10°C/min was shown in figure 5.8. The crystallization temperatures of EVOH/clay nanocomposite films containing different organoclays varied (only 0.4°C standard

deviation). Consequently, the surfactant types, which treated nanoclay, did not significantly affect the crystallization temperatures of EVOH/clay nanocomposite films.

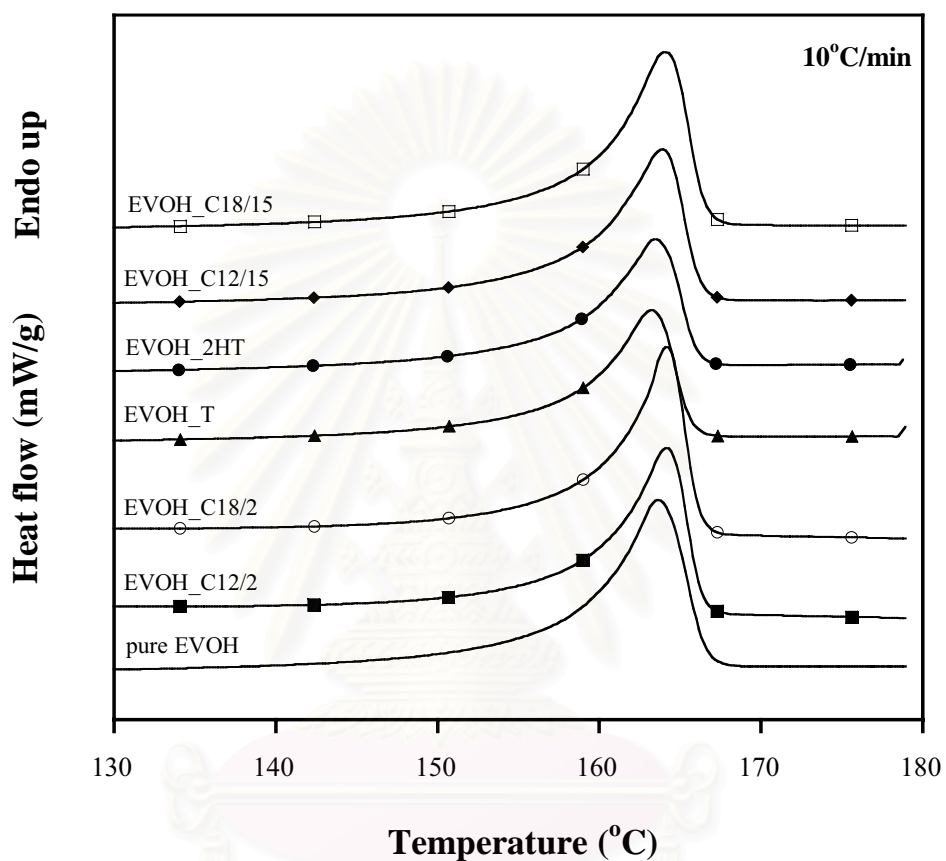


Figure 5.7 DSC melting curves of EVOH/clay nanocomposite films containing 3 wt% organoclays, which were treated with different surfactant types, at heating rate of 10°C/min

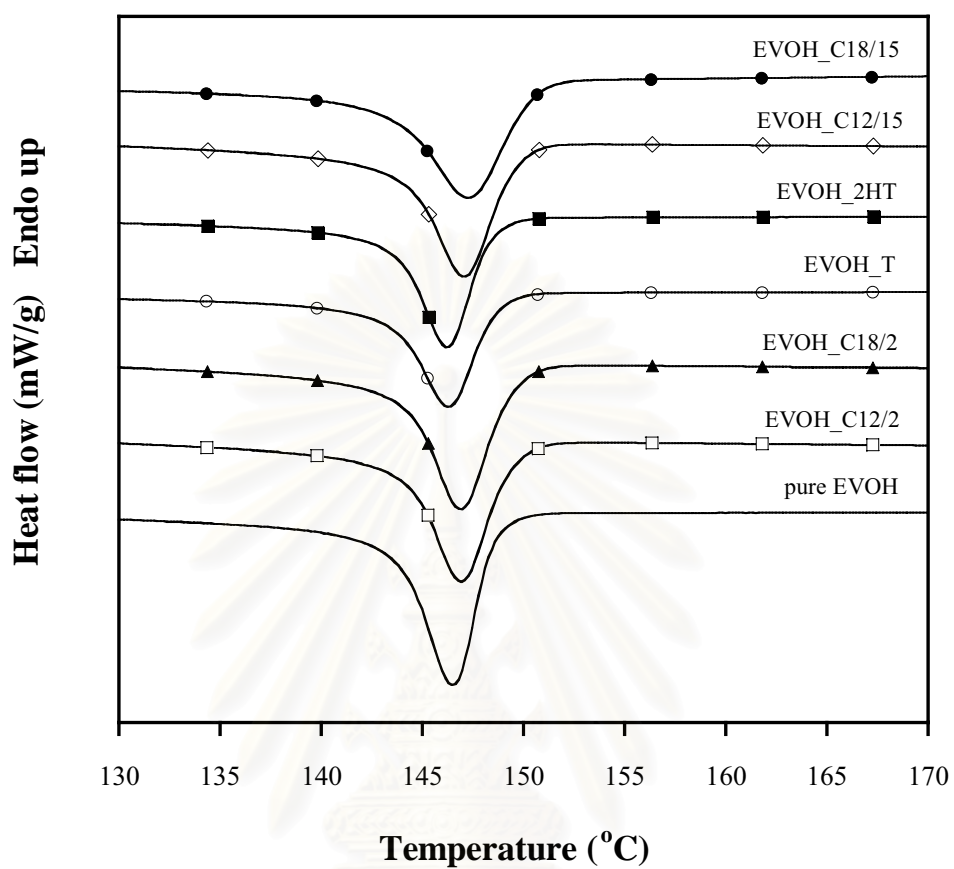


Figure 5.8 DSC cooling curves of EVOH/clay nanocomposite films containing 3 wt% organoclays, which were treated with different surfactant types, at cooling rate of 10°C/min

สถาบันวิทยบริการ
จุฬาลงกรณ์มหาวิทยาลัย

5.1.3 The mechanical properties of EVOH/clay nanocomposite films

The mechanical properties, such as tensile strength, tensile modulus and elongation at break, were determined according to ASTM D882 by Universal testing machine (Instron 5567). The tensile strength of EVOH/clay nanocomposite films was determined as the maximum tensile stress. The tensile modulus was the first linear slope of the stress-strain curve. The elongation at break was determined as the maximum tensile strain at break.

5.1.3.1 Effect of the short (C12) and long (C18) alkyl tail surfactant

Figure 5.9 to 5.11 showed the tensile strength, tensile modulus and elongation at break of EVOH/clay nanocomposite films, respectively, containing 3 wt% MMT_C12/2, MMT_C12/15, MMT_C18/2 and MMT_C18/15 organoclays. Tensile strength of EVOH_C18/2 and EVOH_C18/15 nanocomposite films showed 90% and 18% higher values than EVOH_C12/2 and EVOH_C12/15 films. Tensile modulus of nanocomposite films containing MMT_C18/2 and MMT_C18/15 organoclay showed 94% and 23% higher value than those treated with C12/2 and C12/15 surfactant. Therefore, the nanocomposite films containing long (C18) alkyl chain surfactants showed higher tensile strength and tensile modulus than those treated by short (C12) alkyl chain surfactants, which was in the same trend as the area under XRD peak at $2\theta = 20.4^\circ$. When the degree of crystallinity of nanocomposite films increased, tensile strength and tensile modulus also increased. In addition, the enhancement was caused by inorganic content in EVOH/clay nanocomposite films whose role was reinforcing filler. From figure 5.11, EVOH/clay nanocomposite films containing short (C12) alkyl chain surfactant exhibited similar value of elongation at break as pure EVOH film. In addition, EVOH_C18/2 nanocomposite film showed the highest elongation at break (increased 85% compared to pure EVOH film). However, the elongation at break of EVOH_C18/15 nanocomposite film was 30% lower than that of pure EVOH film, which was a result of too large size of C18/15 surfactant in silicate layers.

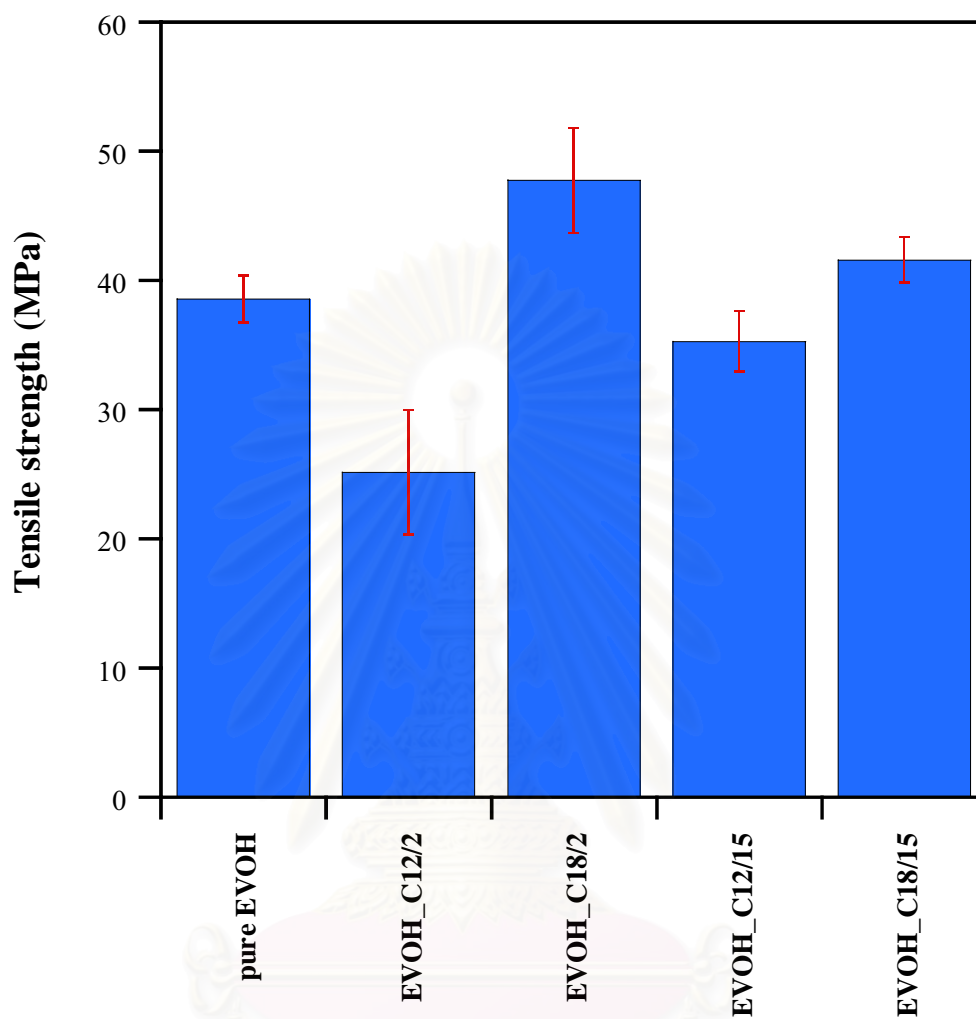


Figure 5.9 Tensile strength of EVOH/clay nanocomposite films containing 3 wt% MMT_C12/2, MMT_C12/15, MMT_C18/2 and MMT_C18/15 organoclays

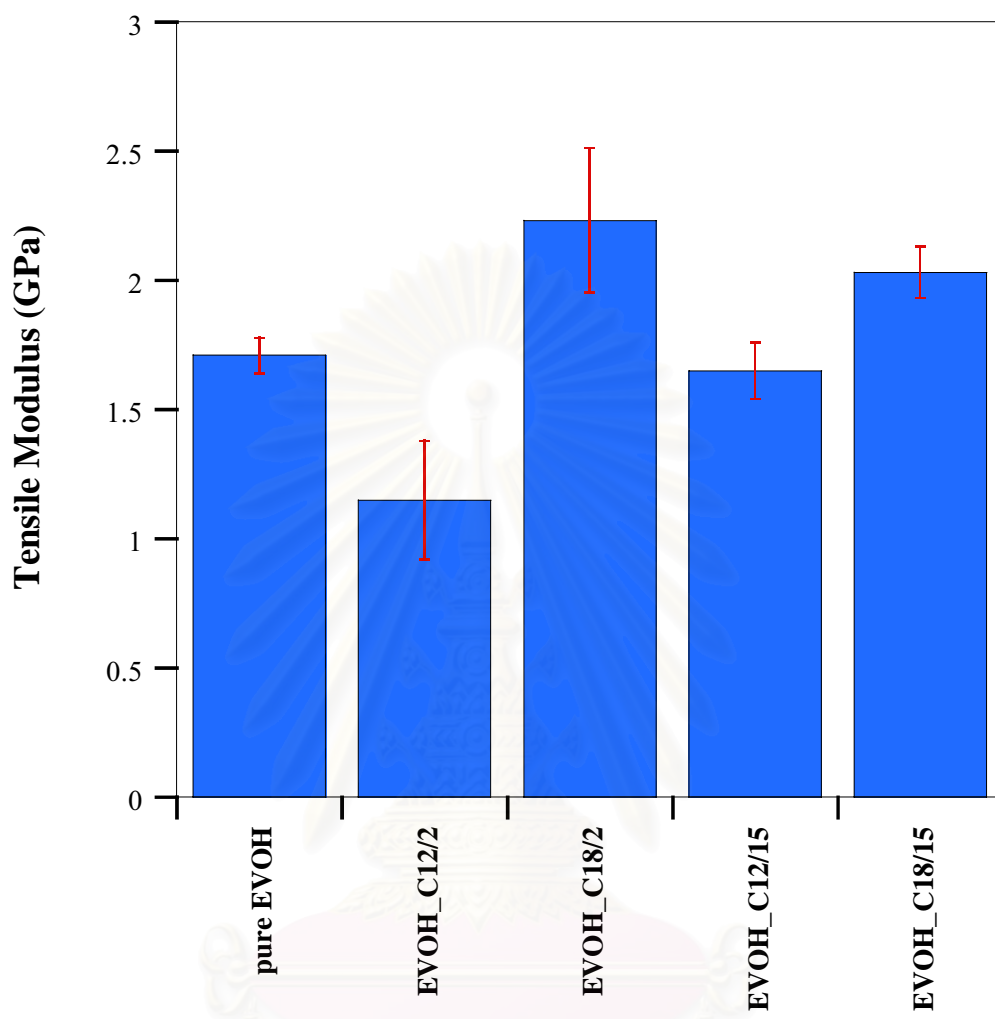


Figure 5.10 Tensile modulus of EVOH/clay nanocomposite films containing 3 wt% MMT_C12/2, MMT_C12/15, MMT_C18/2 and MMT_C18/15 organoclays

จุฬาลงกรณ์มหาวิทยาลัย

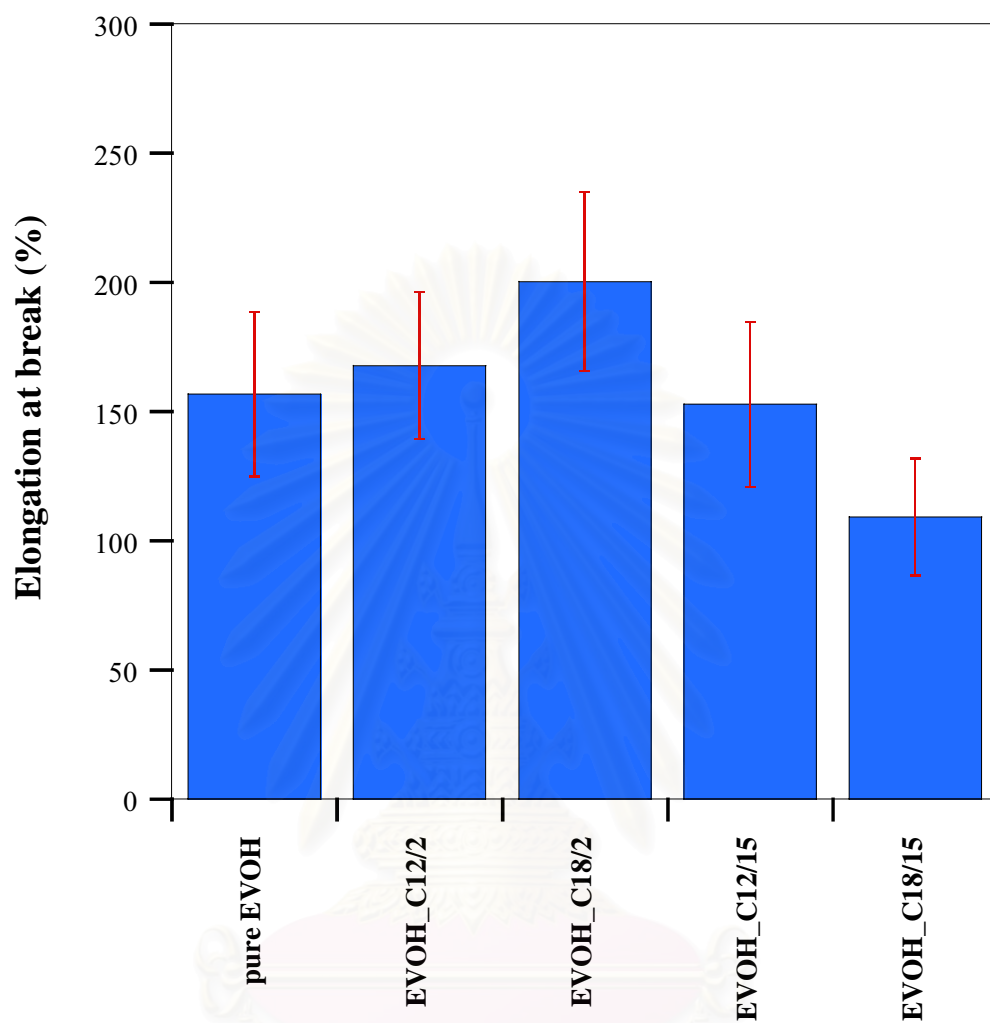


Figure 5.11 Elongation at break of EVOH/clay nanocomposite films containing 3 wt% MMT_C12/2, MMT_C12/15, MMT_C18/2 and MMT_C18/15 organoclays

จุฬาลงกรณ์มหาวิทยาลัย

5.1.3.2 Effect of the number of repeating units of oxyethylene

Figure 5.9 to 5.11 showed tensile strength, tensile modulus and elongation at break of EVOH/clay nanocomposite films, respectively, containing 3 wt% organoclays, which were treated by surfactants containing 2 and 15 repeating units of oxyethylene: C12/2 and C12/15 surfactants, respectively. The EVOH_C12/15 nanocomposite films showed 40% and 43% higher values of tensile strength and tensile modulus, respectively, than that EVOH_C12/2 film. Even though XRD's result showed exfoliated structure of clay in the matrix, the reduction in mechanical properties occurred. The tensile strength and tensile modulus were 35% and 33% lower than those of pure EVOH film. In addition, the EVOH_C12/15 nanocomposite films showed slightly lower tensile strength and tensile modulus compared to pure EVOH. However, tensile strength and tensile modulus of EVOH_C18/2 nanocomposite films were higher than those of EVOH_C18/15 nanocomposite films. This result was caused by the degree of crystallinity of nanocomposite films, quantity of inorganic content in the films and high surface area of organoclay. From XRD's result, EVOH_C18/2 film showed higher degree of crystallinity than EVOH_C18/15. In addition, the clay in EVOH_C18/2 film was intercalated-exfoliated structure which enhanced the interfacial interaction between clay and polymer matrix. This was a result of the molecular size of surfactant. The large molecular size of C18/15 surfactant caused the difficulty of orientation which was indicated by the decrease in degree of crystallinity of EVOH. Consequently, the tensile strength and tensile modulus of EVOH_C18/15 nanocomposite films were lower than those treated by C18/2 surfactant. The elongation at break of EVOH_C12/2 nanocomposite films were the same as those treated with C12/15 surfactant. However, in case of long (C18) alkyl chain surfactant, the elongation at break of EVOH_C18/2 films was higher than those treated with C18/15 surfactant. This could be due to the disorder of silicate layers of clay in EVOH/clay nanocomposite films which was confirmed by XRD technique.

5.1.3.3 Effect of the number of alkyl tail surfactant

Figure 5.12 to 5.14 showed the tensile strength, tensile modulus and elongation at break of EVOH/clay nanocomposite films, respectively, containing 3 wt% MMT_T and MMT_2HT organoclays. The tensile strength, tensile modulus and elongation at break of EVOH_T nanocomposite films showed 19, 14 and 34%, respectively, higher value than those treated by 2HT surfactant and 51%, 35% and 51% higher values than pure EVOH films, respectively.

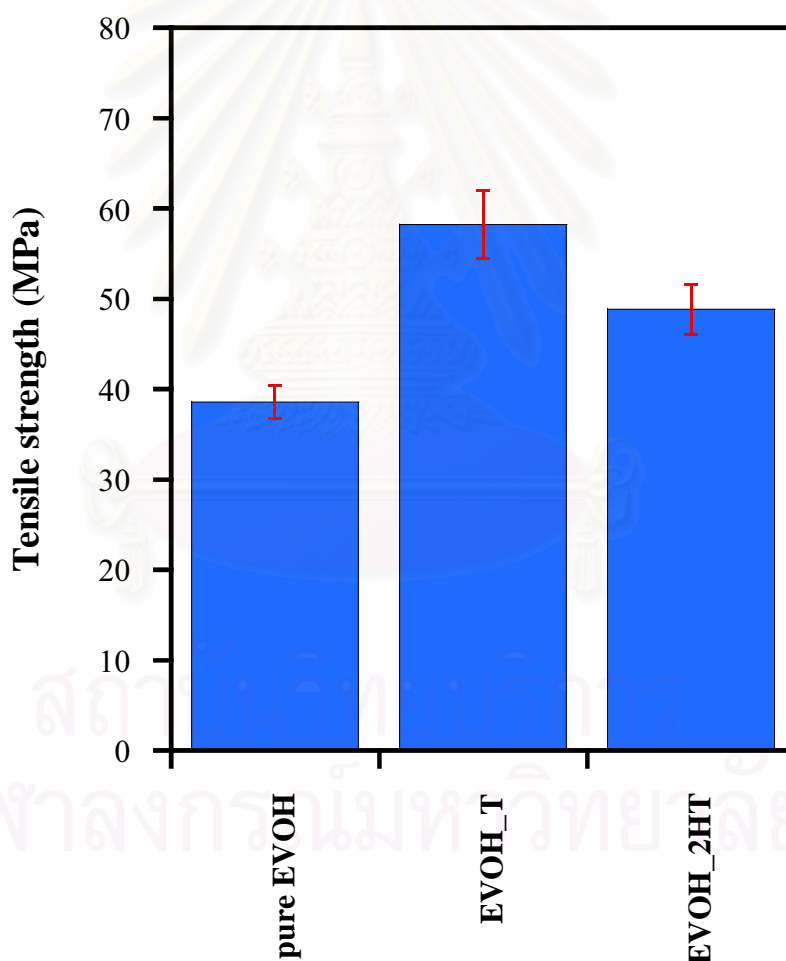


Figure 5.12 Tensile strength of EVOH/clay nanocomposite films containing 3 wt% MMT_T and MMT_2HT organoclays

From XRD result, the degree of crystallinity of EVOH_T nanocomposite films was higher than those containing two alkyl tails surfactant. In addition, the quantity of inorganic content in EVOH_T nanocomposite films was higher than EVOH_2HT nanocomposite films. Therefore, the more inorganic content and higher degree of crystallinity of the films enhanced mechanical properties of EVOH_T films.

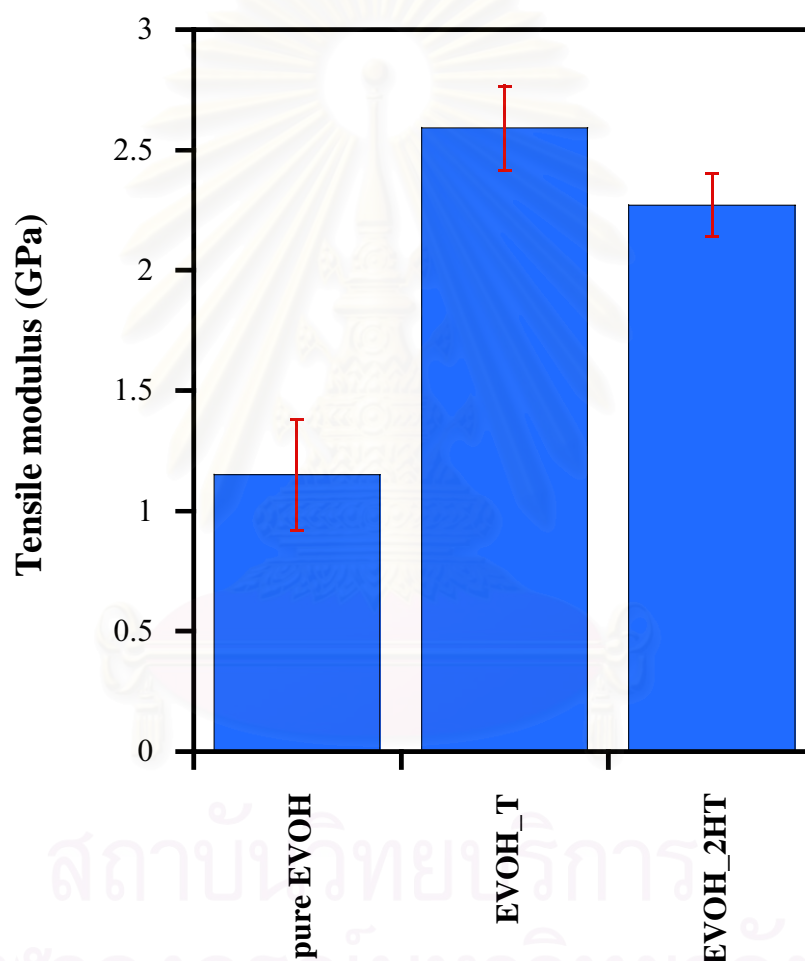


Figure 5.13 Tensile modulus of EVOH/clay nanocomposite films containing 3 wt% MMT_T and MMT_2HT organoclays

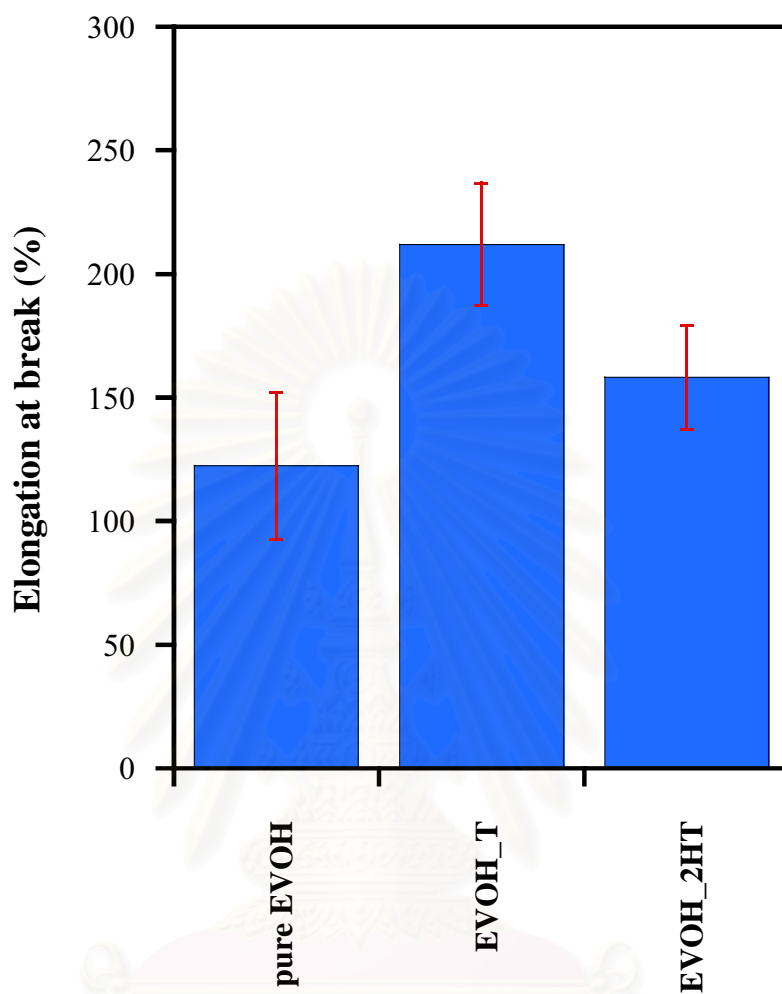


Figure 5.14 Elongation at break of EVOH/clay nanocomposite films containing 3 wt% MMT_T and MMT_2HT organoclays

สถาบันวิทยบริการ
จุฬาลงกรณ์มหาวิทยาลัย

5.1.4 The oxygen transmission rate (O_2TR) of EVOH/clay nanocomposite films

The oxygen permeation of EVOH/clay nanocomposite films was determined by MOCON OX-TRAN® 2/21 according to ASTM D3985. The samples were tested at 23°C, 1 atm and 0 % RH (dry condition).

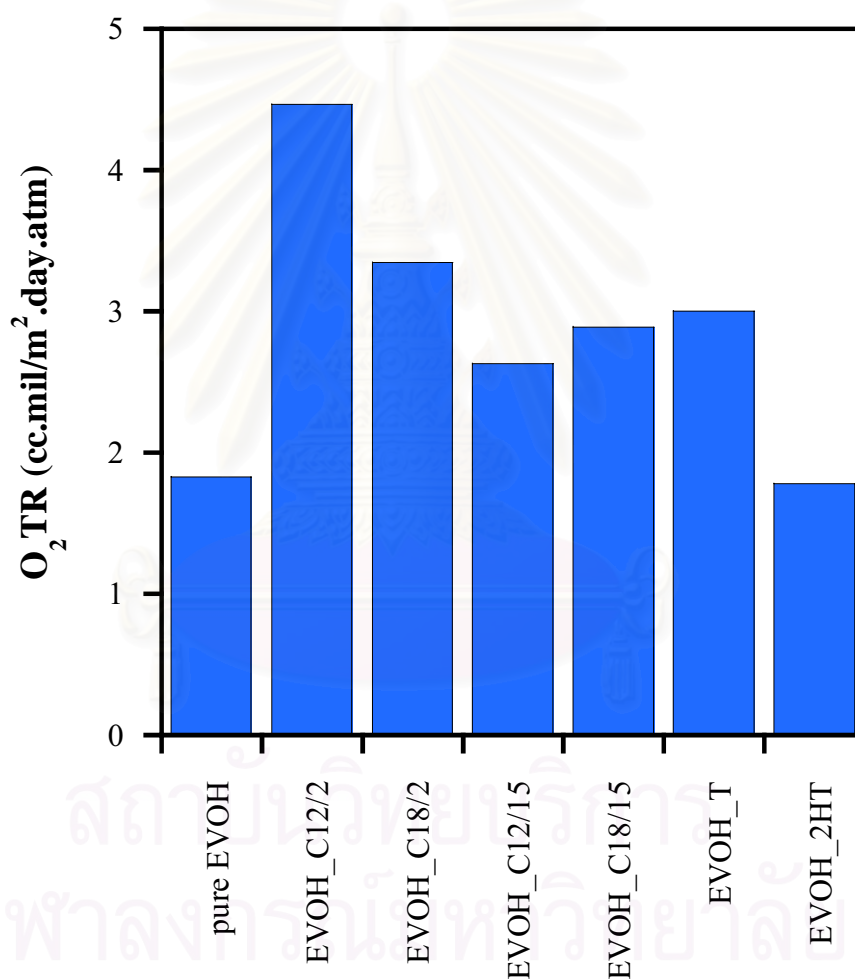


Figure 5.15 Oxygen transmission rates (O_2TR) of EVOH/clay nanocomposite films containing 3 wt% organoclays, 23°C, 1 atm and 0 % RH.

Table 5.1 The relationship between the degree of clay dispersion in EVOH matrix and the oxygen transmission rate of EVOH/clay nanocomposite films containing 3 wt% different organoclays

EVOH/clay nanocomposite film	Degree of clay dispersion in EVOH matrix	ΔC^*	O ₂ TR (cc.mil/m ² .day.atm)
Pure EVOH		1.00	1.8243
EVOH_C12/2	Exfoliated	0.56	4.4605
EVOH_C18/2	Intercalated- exfoliated	1.11	3.3424
EVOH_C12/15	Intercalated- exfoliated	0.61	2.6270
EVOH_C18/15	Intercalated	0.88	2.8886
EVOH_T	Intercalated	1.82	N/A
EVOH_2HT	Conventional composite	1.15	1.7770

Note: $^* \Delta C = \frac{\% \text{ Crystallinity}_{\text{nanocomposite}}}{\% \text{ Crystallinity}_{\text{pure EVOH}}} = \text{relative degree of crystallinity}$

Figure 5.15 showed the oxygen transmission rate of EVOH/clay nanocomposite films containing 3 wt% organoclays, at 23°C, 1 atm and 0 % RH. The oxygen transmission rates of all EVOH/clay nanocomposite films increased compared to pure EVOH film except EVOH_2HT film. In addition, EVOH_2HT, EVOH_C18/15 and EVOH_T films, whose clay structures were conventional composite and intercalated nanocomposite, showed lower values of O₂TR than intercalated-exfoliated and exfoliated films which were EVOH_C18/2 and EVOH_C12/2, respectively, as shown in Table 5.1. This result was caused by the agglomeration of clay in EVOH matrix and micro-size of clay particle, confirmed by rough surfaces, which were determined by touching and appearance.

5.2 Effect of organoclay loading on EVOH/clay nanocomposite films properties.

From previous research, the organoclay loading, which was added into polymer matrix in order to form nanocomposite, affected the properties of polymer/clay nanocomposites such as mechanical, thermal and gas barrier properties [23-25,32]. Therefore, the effect of organoclay loading on mechanical, thermal and gas barrier properties of EVOH/clay nanocomposite films was studied.

5.2.1 Degree of clay dispersion and degree of crystallinity of EVOH_T nanocomposite films

Figure 5.16 showed the X-ray diffraction patterns of EVOH/clay nanocomposite films with different MMT_T organoclay loading. The nanocomposite films containing 1 wt% MMT_T organoclay did not show peak, in which means nearly exfoliated state occurred. However, this result might be due to the low quantity of organoclay. The 3, 5 and 7 wt% nanocomposite films showed nearly the same diffraction (001) angle value at 2.67, 2.73 and 2.66°, corresponding to an interlayer spacing of clay of 3.31, 3.24 and 3.32 nm, respectively. However, the diffraction peak showed an increase in the intensity as a function of organoclay loading. In other word, the order of silicate layer of clay in EVOH_T nanocomposite films increased with increasing organoclay loading, which indicated the intercalated structure in nanocomposite. This could be due to the quantity of organoclay. Moreover, it indicated that the EVOH chains intercalated into the interlayer spacing of clay when organoclay were treated by one alkyl tail surfactant. Figure 5.17 showed the X-ray diffraction patterns of EVOH/clay nanocomposite films containing different MMT_T organoclay loading, at $2\theta = 17-24^\circ$. The XRD peaks at 20.4° of EVOH and EVOH_T nanocomposite film, which contained different organoclay loading, corresponded to orthorhombic crystal structure of polymer. Consequently, the quantity of organoclay did not affect crystal structure of EVOH_T nanocomposite film. Moreover, the area under diffraction peak indicated the degree of crystallinity of nanocomposite film. The change of degree of

crystallinity of EVOH/clay nanocomposite films depended on organoclay loading. The 1 wt% nanocomposite film showed 63% decrease in the degree of crystallinity, compared to pure EVOH film. However, the degree of crystallinity of nanocomposite films increased with increasing organoclay loading and slightly decreased when the organoclay loading was higher than 5 wt% organoclay (data was shown in Table F.2).

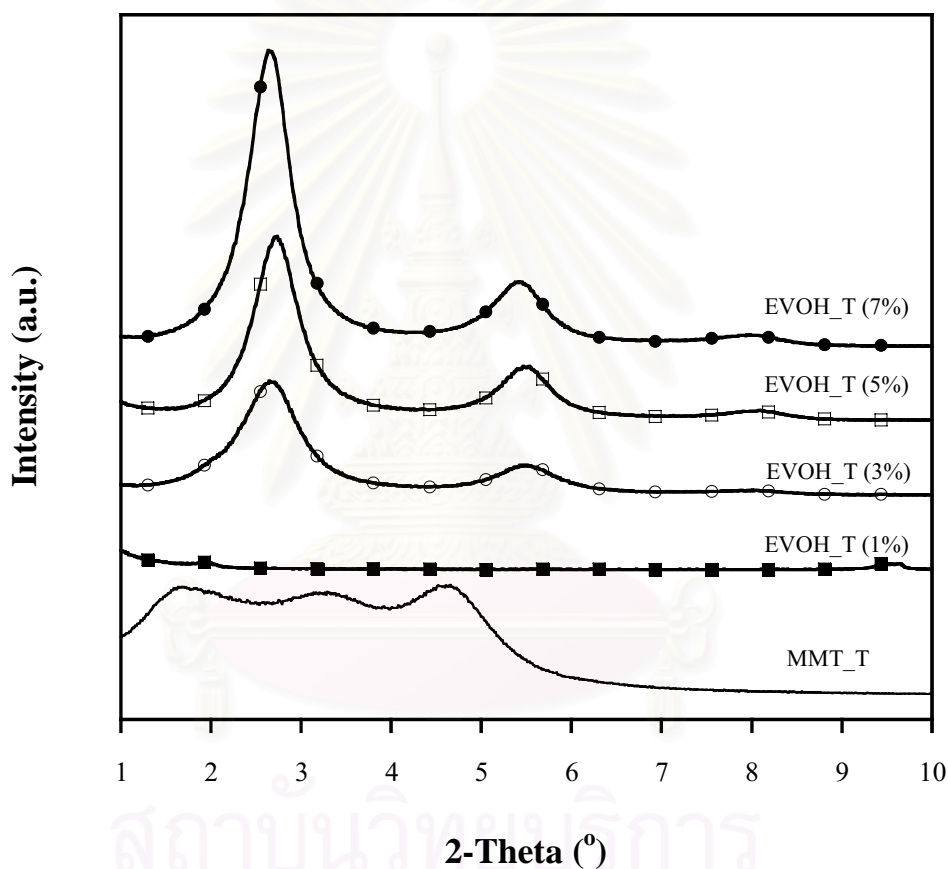


Figure 5.16 X-ray diffraction patterns of EVOH/clay nanocomposite films with different MMT_T organoclay loading, at $2\theta = 1-10^\circ$.

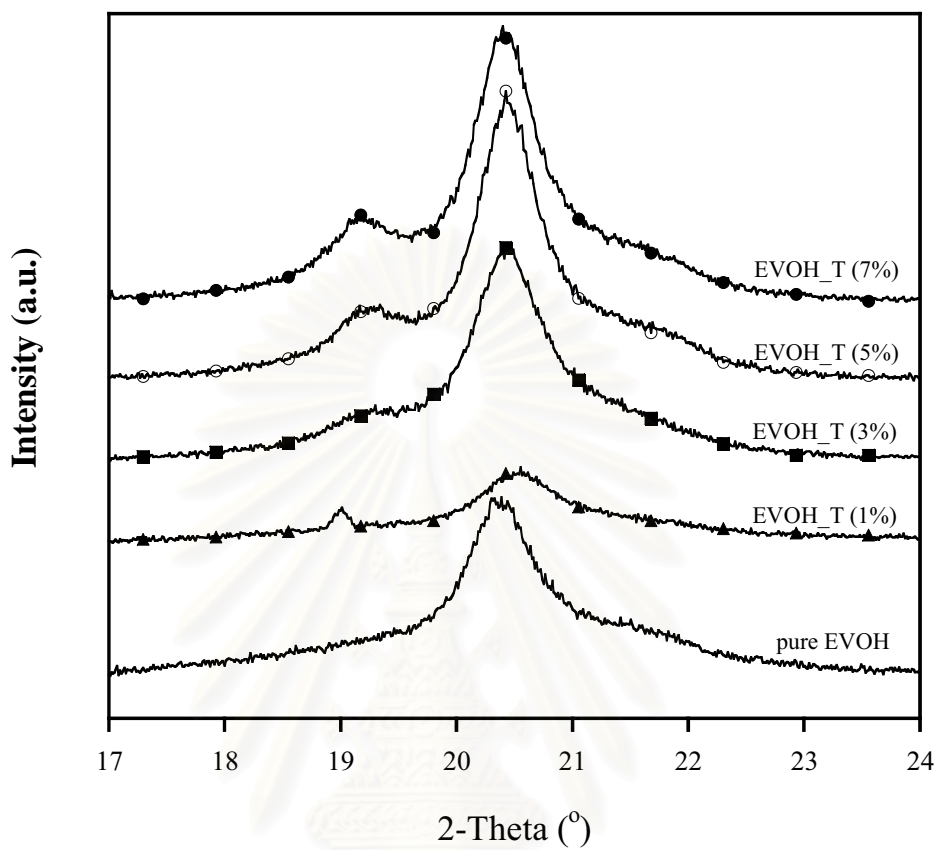


Figure 5.17 X-ray diffraction patterns of EVOH/clay nanocomposite films with different MMT_T organoclay loadings, at $2\theta = 17\text{-}24^\circ$.

สถาบันวิทยบริการ
จุฬาลงกรณ์มหาวิทยาลัย

5.2.2 Thermal properties of EVOH_T nanocomposite films

Figure 5.18 showed the DSC melting profiles of EVOH/clay nanocomposite films with different MMT_T organoclay loadings, at heating rate of 10°C/min. The crystalline-melting temperature (T_m) of nanocomposite films slightly decreased with increasing organoclay loading. Therefore, the organoclay loading did not significantly affect the T_m of EVOH_T nanocomposite film. In addition, increasing organoclay loading decreased area under melting peak, indicating the decrease of the degree of crystallinity in nanocomposite films. The DSC cooling curves of EVOH/clay nanocomposite films with different MMT_T organoclay loadings, at cooling rate of 10°C/min, was shown in figure 5.19. The crystallization temperatures (T_c) of nanocomposite films slightly increased compared to pure EVOH. However, it slightly decreased with increasing organoclay loading. This result was consistent with cooling rate at 5 and 20°C/min of films. Consequently, the organoclay loading also did not significantly affect the T_c of EVOH_T nanocomposite film.

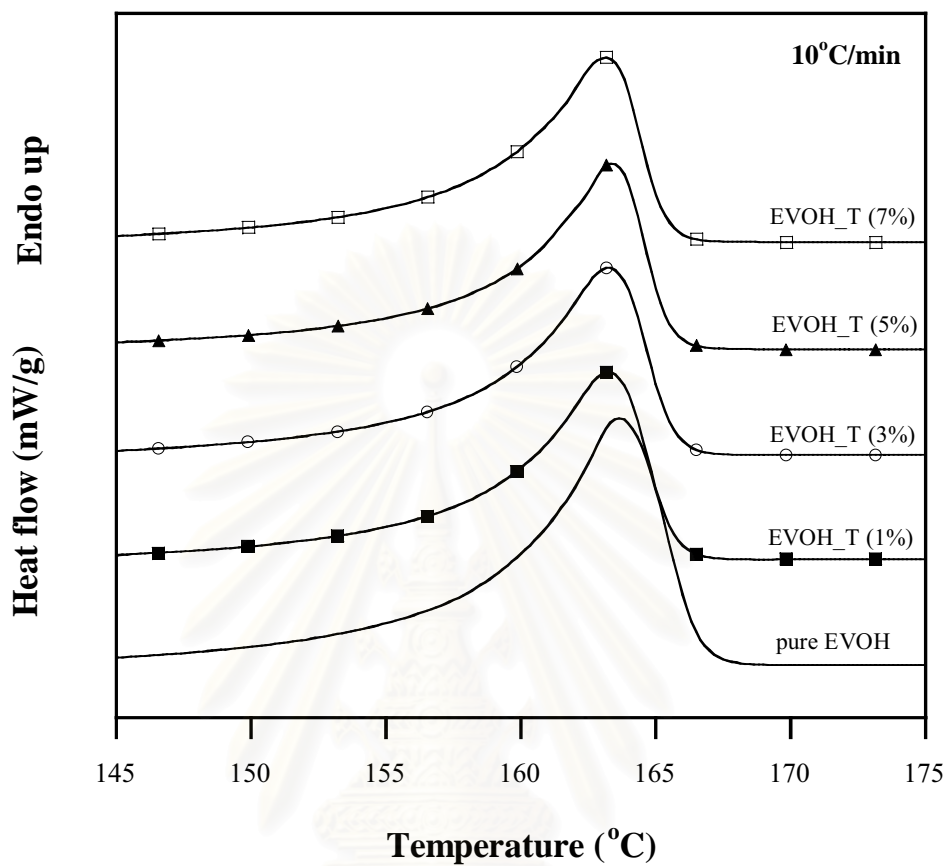


Figure 5.18 DSC melting curves of EVOH/clay nanocomposite films containing MMT_T organoclay, at heating rate of 10°C/min.

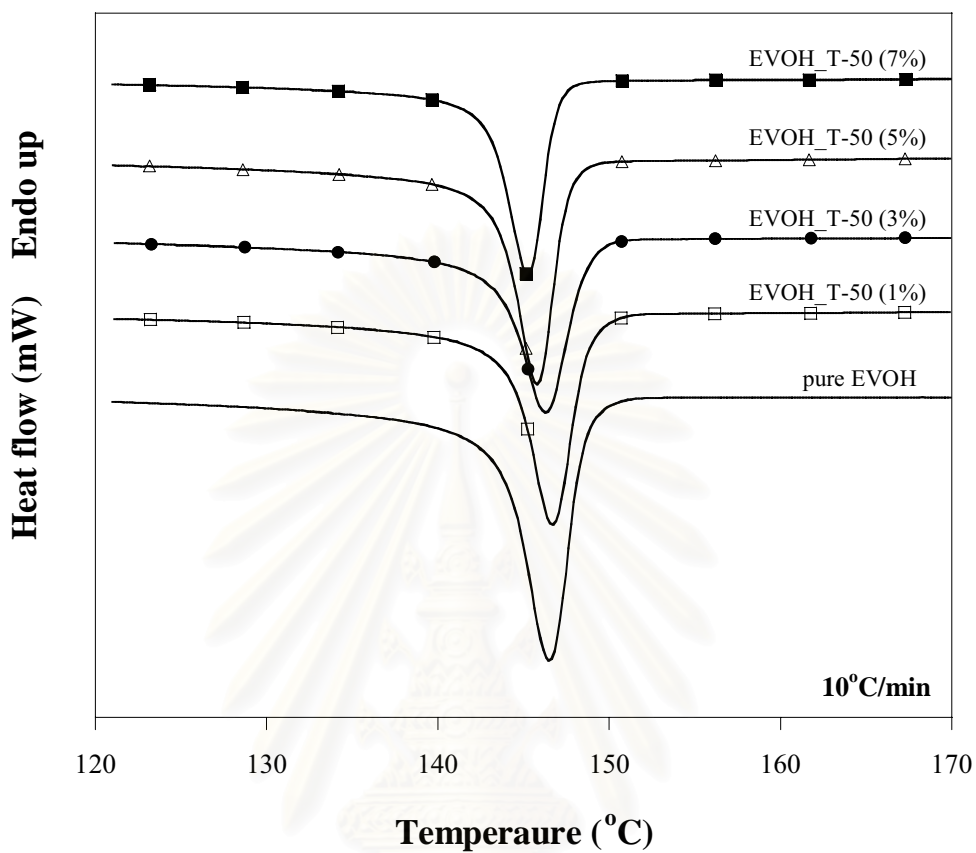


Figure 5.19 DSC cooling curves of EVOH/clay nanocomposite films containing MMT_T organoclay, at cooling rate of 10°C/min.

สถาบันวิทยบริการ
จุฬาลงกรณ์มหาวิทยาลัย

5.2.3 The mechanical properties of EVOH_T nanocomposite films

Figure 5.20 and 5.21 showed the relationship between the mechanical properties; i.e., tensile strength, elongation at break and tensile modulus, respectively, of EVOH/clay nanocomposite films containing different MMT_T organoclay loading (1, 3, 5 and 7 wt%). Tensile strength of EVOH/clay nanocomposite films increased with increasing organoclay loading from 0 up to 3 wt% (increased 51%) and decreased when the organoclay loading was higher than 3 wt%. Tensile modulus of nanocomposite films slightly increased with 1 wt% organoclay (increased 5%) and significantly increased with 3 wt% organoclay (increased 52%, compared to pure EVOH). When the organoclay loading was higher than 3 wt%, tensile modulus decreased. However, tensile modulus of all nanocomposite films was higher than that of pure EVOH film. The increase of tensile strength and tensile modulus was caused by the inorganic content in EVOH_T nanocomposite films. The degree of crystallinity of nanocomposite film was another factor of these mechanical properties enhancement. From figure 5.20, the nanocomposite films containing 1 wt% MMT_T showed the highest elongation at break (increased 42%) compared to pure EVOH. But the elongation at break of nanocomposite films was slightly decreased with increasing organoclay loading. This result was caused by the order of silicate layers of clay in EVOH_T nanocomposite films.

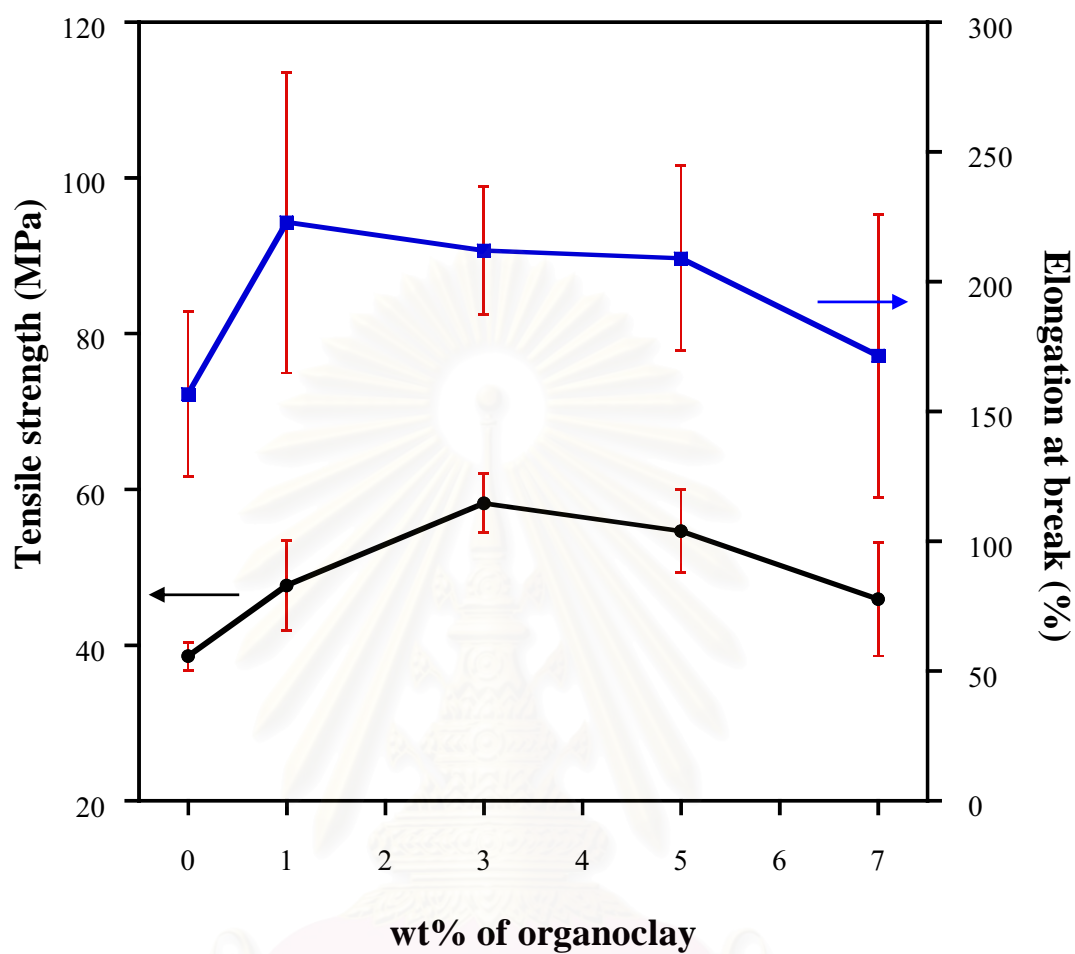


Figure 5.20 Tensile strength and elongation at break of EVOH/clay nanocomposite films containing different MMT_T organoclay loading

สถาบันวิทยบริการ
จุฬาลงกรณ์มหาวิทยาลัย

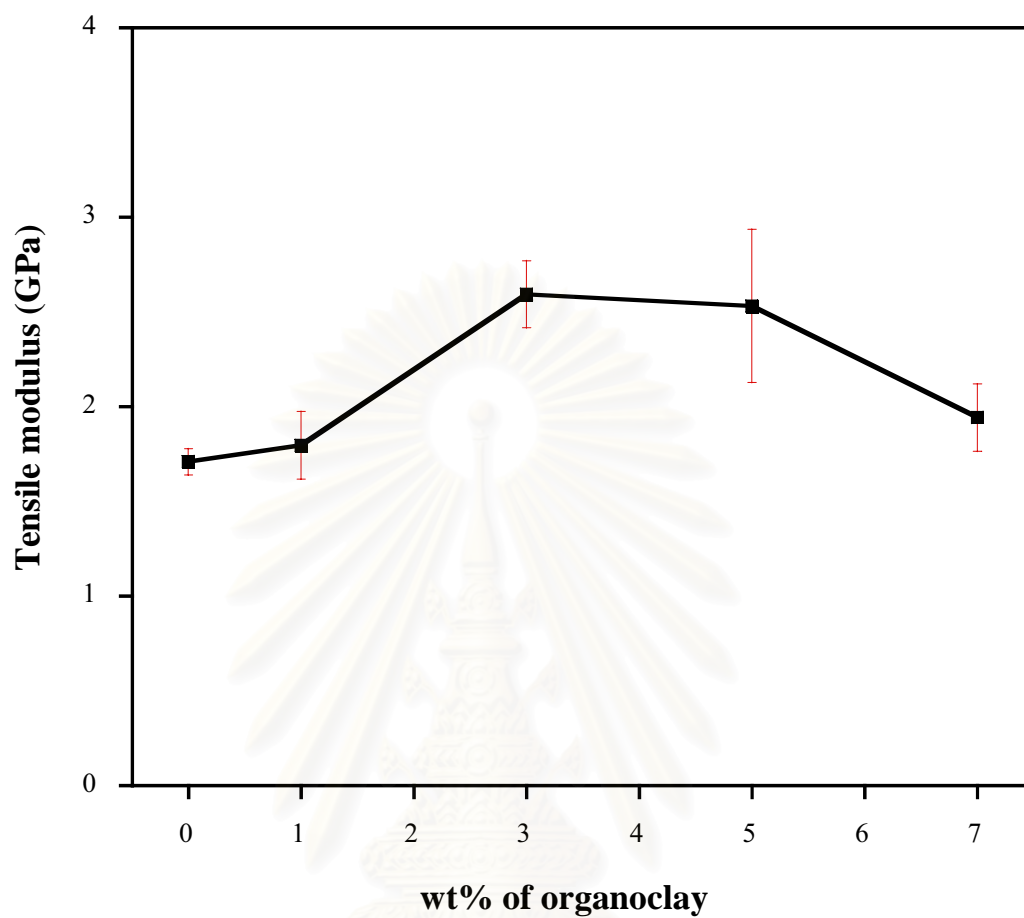


Figure 5.21 Tensile modulus of EVOH/clay nanocomposite films containing different MMT_T organoclay loading

สถาบันวิทยบริการ
จุฬาลงกรณ์มหาวิทยาลัย

5.2.4 The oxygen transmission rate (O_2TR) of EVOH_T nanocomposite films

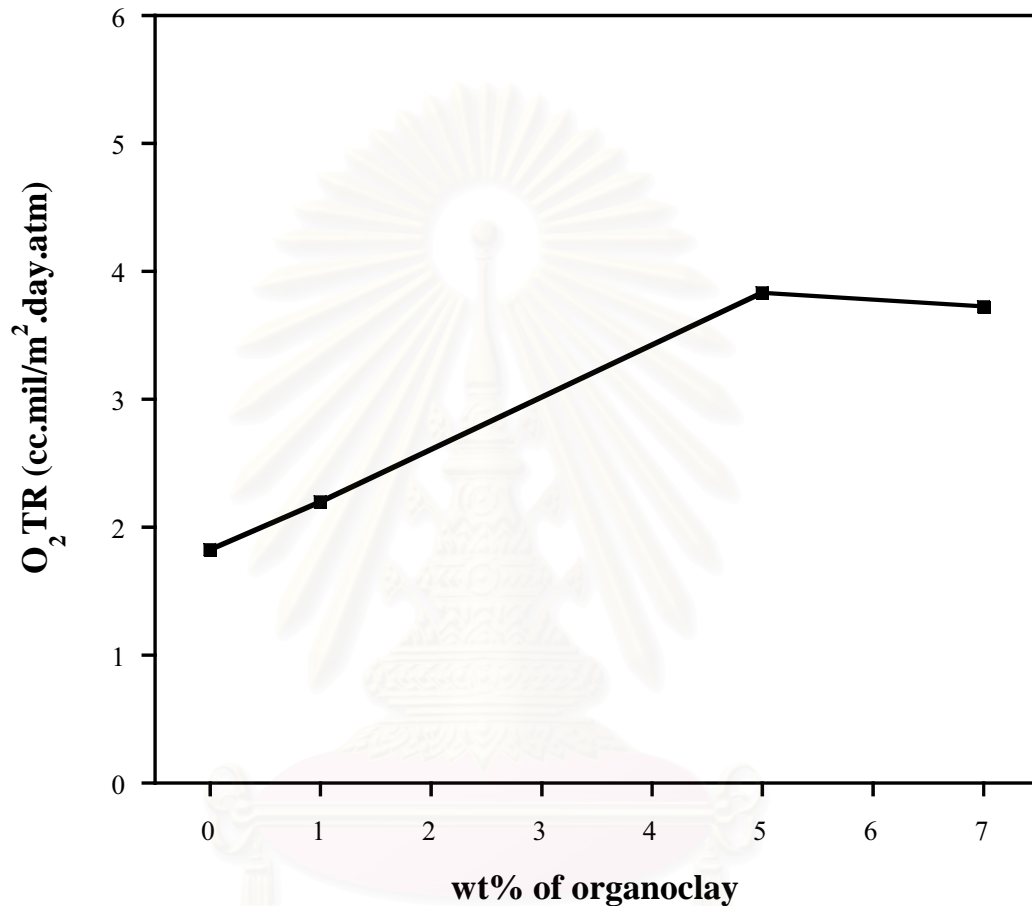


Figure 5.22 Oxygen transmission rate of EVOH/clay nanocomposite films containing different MMT_T organoclay loading, at 23°C, 1 atm and 0 % RH.

Figure 5.22 showed the oxygen transmission rate (O_2TR) of EVOH/clay nanocomposite films containing different MMT_T organoclay loading, at 23°C, 1 atm and 0 %RH (dry condition). Oxygen transmission rate of EVOH/clay nanocomposite films increased compared to pure EVOH. In addition, O_2TR increased with increasing organoclay loading. This result was caused by the agglomeration of clay in EVOH matrix and micro-size of clay particle, confirmed by rough surfaces, which were determined by touching and appearance.

CHAPTER VI

CONCLUSIONS

In this study, ethylene vinyl alcohol (EVOH) copolymers were improved their properties, such as mechanical, thermal and gas barrier properties, by mixing with the small amount of nanoclay. EVOH/clay nanocomposite films were prepared by blown film twin screw extruder. The effect of surfactants on the degree of clay dispersion of nanocomposite films was determined. In addition, the effect of surfactant and organoclay loading on mechanical, thermal and gas barrier properties of nanocomposite films were also studied.

Tensile strength and tensile modulus of EVOH/clay nanocomposite films were increased due to increasing the degree of crystallinity, which was determined by XRD technique. In addition, the increase of tensile strength and tensile modulus was resulted by the quantity of inorganic in nanocomposite film. Therefore, the addition of organoclay into EVOH matrix increased the stiffness of material. EVOH/clay nanocomposite films containing long (C18) alkyl tail and one alkyl tail surfactants had better properties than those with short (C12) alkyl chain and two alkyl tail surfactant, respectively. In addition, the EVOH/clay nanocomposite films containing short (C12) alkyl tail surfactants reduced the degree of crystallinity. It led to decrease their mechanical properties such as tensile strength and tensile modulus. The permeability of oxygen of EVOH/clay nanocomposite films increased compared to pure EVOH film except EVOH_2HT film. In addition, O₂TR increased with increasing organoclay loading. This result could be due to the agglomeration of clay in EVOH matrix and micro-size of clay particle. The EVOH/clay nanocomposite films containing 3 wt% MMT_T organoclay showed the highest tensile strength and tensile modulus. In addition, the nanocomposite films containing 1 wt% MMT_T organoclay showed the highest elongation at break but it was only 4.88 percent better

than those containing 3 wt% MMT_T organoclay. Therefore, 3 wt% MMT_T organoclay were suitable for improving EVOH/clay nanocomposite films.



สถาบันวิทยบริการ
จุฬาลงกรณ์มหาวิทยาลัย

REFERENCES

- [1] Kuntz, L. A. Food product: Material differences [Online]. Available from:
<http://www.foodproductdesign.com/archive/1992/0292PK.html>
- [2] Advanced plastic films for functional packaging (1) oxygen barrier films
[Online]. Available from: http://www.film-sheet.com/en/13front_old/topics/12.html
- [3] Garland, A. Nanotechnology in plastic packaging. UK: Pira International, 2004.
- [4] Pinnavaia, T. J. and Beall, G. W. Polymer-clay nanocomposites. New York: John Wiley & Sons, 2001.
- [5] Muramatsu, M.; Okura, M.; Kuboyama, K.; Ougizawa, T.; Yamamoto, T.; Nishihara, Y.; Saito, Y.; Ito, K.; Hirata, K. and Kobayashi, Y. Oxygen permeability and free volume hole size in ethylene-vinyl alcohol copolymer film: temperature and humidity dependence. Radiation Physics and Chemistry 68 (2003) : 561-564.
- [6] Gao, F. Clay/polymer composites: the story. Materialstoday (2004): 50-55.
Available from: <http://www.olmix.com>
- [7] Lopez-Rubio, A.; Lagaron, J. M.; Gimenez, E.; Cava, D.; Hernandez-Munoz, P.; Yamamoto, T. and Gavara, R. Morphological alterations induced by temperature and humidity in ethylene-vinyl alcohol copolymers. Macromolecules 36 (2003) : 9467-9476.
- [8] What Are EVAL™ Resins? [Online]. Available from: <http://www.eval.be>
[2005, Dec 10]
- [9] Barrier Films- An Overview [Online]. Available from:
<http://www.keepsafe.ca/barrier.shtml>
- [10] Armstrong, R. B. Effect of polymer structure on gas barrier of ethylene vinyl alcohol (EVOH) and considerations for package development
[Online]. Available from: <http://www.eval.be>
- [11] <http://www.cheng.es.osaka-u.ac.jp>
- [12] Hay J. N. and Shaw S. J. Clay-Based Nanocomposites [Online]. Available from: <http://www.azom.com/details.asp?ArticleID=936>

- [13] New EVOH barrier resin [Online]. Available from:
<http://www.kuraray.co.jp/en/products/ex.html>
- [14] Unique NRC-Industry Research Partnership Launched [Online]. Available from: http://www.nrc-cnrc.gc.ca/highlights/2003/0307nanocomp_e.html
- [15] Twin screw extrusion [Online]. Available from:
<http://www.polymerprocessing.com/operations/tscrew/index.html>
- [16] Blown film [Online]. Available from:
http://www.bpf.co.uk/bpfindustry/process_plastics_blow_n_film.cfm
- [17] Extrusion [Online]. Available from: <http://www.pct.edu/prep/ex.html>
- [18] Tensile property testing of plastics [Online]. Available from:
<http://www.matweb.com/reference/tensilestrength.asp>
- [19] X-ray Technique Laboratory [Online]. Available from:
http://www.mtec.or.th/th/labs/xrd&xrf/about_en.html
- [20] Differential scanning calorimetry [Online]. Available from:
<http://pslc.ws/macrog/dsc.htm>
- [21] Differential Scanning Calorimetry (DSC) [Online]. Available from:
<http://www.mrl.ucsb.edu/mrl/centralfacilities/polymer/DSC.html>
- [22] Fornes, T. D.; Yoon, P. J.; Hunter, D. L.; Keskkula, H. and Paul, D. R. Effect of organoclay structure on nylon 6 nanocomposite morphology and properties. Polymer 43 (2002) : 5915-5933.
- [23] Ke, Z. and Yongping, B. Improve the gas barrier property of PET film with montmorillonite by in situ interlayer polymerization. Materials Letters 59 (2005) : 3348-3351.
- [24] Frounchi, M.; Dadbin, S.; Salehpour, Z. and Noferesti, M. Gas barrier properties of PP/EPDM blend nanocomposites. Journal of Membrane Science 282 (2006) : 142-148.
- [25] Liu, T. X.; Liu, Z. H.; Ma, K. X.; Shen, L.; Zeng, K. Y. and He, C. B. Morphology, thermal and mechanical behavior of polyamide 6/layered-silicate nanocomposite. Composites Science and Technology 63 (2003) : 331-337.

- [26] Ratna, D.;Divekar, S.;Samui, A. B.;Chakraborty, B. C. and Banthia, A. K. Poly(ethylene oxide)/clay nanocomposite: Thermomechanical properties and morphology. Polymer 47 (2006) : 4068–4074.
- [27] Artzi, N.;Nir, Y.;Wang, D. and Narkis, M. EVOH/clay nanocomposites produced by melt processing. Polymer Composites 22 (2001) : 710-720.
- [28] Artzi, N.;Nir, Y.;Narkis, M. and Siegmann, A. Melt blending of ethylene vinyl alcohol copolymer/clay nanocomposites: Effect of the clay type and processing conditions. Polymer Science 40 (2002) : 1741-1753.
- [29] Froio, D.;Lucciarini, J.;Thellen, C. and Ratto, J. A. Nanocomposites research for combat ration packaging. 25th Army science conference, 2004.
- [30] <http://surface.akzonobelusa.com>
- [31] Fornes, T. D.;Yoon, P. J.;Hunter, D. L.;Keskkula, H. and Paul, D. R. Effect of organoclay structure on nylon 6 nanocomposite morphology and properties. Polymer 43 (2002) : 5915-5933.
- [32] Ha, S. R.;Ryu, S. H.;Park, S. J. and Rhee, K. Y. Effect of clay surface modification and concentration on the tensile performance of clay/epoxy nanocomposites. Materials Science and Engineering A 448 (2006) : 264-268.
- [33] Limpanart, S. Surface modification of montmorillonite for polymer-clay nanocomposite preparation. Dissertation of Chulalongkorn University, Thailand, 2003.
- [34] Cerrada, M. L.;Perez, E.;Perena, J. M. and Benavente, R. Wide-angle x-ray diffraction study of the phase behavior of vinyl alcohol-ethylene copolymers. Macromolecules 31 (1998) : 2559-2564.



APPENDICES

สถาบันวิทยบริการ
จุฬาลงกรณ์มหาวิทยาลัย

APPENDIX A

Determination of Surfactant Loading

The ion exchange with organic cation (surfactant) was the one of alternative methods for the treatment of clay. Surfactant loading was calculated as follows:

$$g_{surf.} = \frac{CEC \times conc. \times Mw \times kg_{clay}}{\% assay}$$

Where

- $g_{surf.}$ = Weight of surfactant ($g_{surf.}$)
- CEC = Cation exchange capacity of untreated clay (meq/ g_{clay})
- conc. = Concentration of surfactant ($mmol_{surf.}$)
- Mw = Molecular weight of surfactant ($g_{surf.}/mol_{surf.}$)
- kg_{clay} = Weight of untreated clay (kg_{clay})
- % assay = Effectiveness of surfactant

For example: the preparation of organoclay based on Ethoquad 18/25 at 1.0 CEC by using 400 g of clay (CEC of clay = 90 meq/100 g of clay), showing as follow:

$$\text{Surfactant loading} = \frac{0.9 \times 1.0 \times 979.5 \times 0.4}{0.95}$$

$$= 371.1789 \text{ g}$$

สถาบันวิทยบริการ
จุฬาลงกรณ์มหาวิทยาลัย

APPENDIX B

Calculation of Interlayer Spacing of Silicate Layers of Clay

The interlayer spacing of clay and organoclay (or degree of clay dispersion) is calculated by the Bragg's equation. Bragg's law is derived by physicists W.H. Bragg and his son. It was determined the spacing between the planes in the atomic lattice by following equation:

$$n\lambda = 2d \sin \theta$$

- where
- n = Peaks correspond to the {001} basal reflection (n=1)
 - λ = The wavelength of the X-ray radiation used in the diffraction experiment (angstroms), which equals to 1.542 Å when CuK α was used.
 - d = The spacing between the planes in the atomic lattice (Å)
 - θ = The angle between the incident ray and the scattering planes (degrees)

Diffraction angle of organoclay powder and nanocomposite films was determined by X-ray diffraction (XRD). For example, 2 θ peak of MMT_O/12PG was 2.05° which interlayer spacing of organoclay can be calculated as follow:

$$(1)(1.542) = 2d \sin (2.05/2)$$

$$d = 43.1 \text{ \AA}$$

Table B.1 The degree of clay dispersion of organoclays and EVOH/clay nanocomposite films containing 3 wt% different organoclays

	2 θ = 1-10°		2 θ = 11-29°
	2 θ position (°)	degree of clay dispersion (nm)	2 θ position (°)
MMT	7.15	1.23	-
MMT_C18/2	2.05	4.31	-
MMT_T	1.67	5.27	-
MMT_2HT	2.45	3.60	-
MMT_C12/15	2.68	3.29	-
MMT_C18/15	2.52	3.51	-
Pure EVOH	-	-	20.34
EVOH_C12/2	2.00	4.42	20.55
EVOH_C18/2	2.72	3.24	20.39
EVOH_T	2.70	3.27	20.44
EVOH_2HT	2.46	3.59	20.42
EVOH_C12/15	2.87	3.08	20.47
EVOH_C18/15	2.64	3.34	20.38

Table B.2 The degree of clay dispersion of EVOH/clay nanocomposite films containing different MMT_T organoclay loading

EVOH_T nanocomposite films			
MMT_T Organoclay loading	$2\theta = 1-10^\circ$		$2\theta = 11-29^\circ$
	2θ position ($^\circ$)	degree of clay dispersion (nm)	2θ position ($^\circ$)
Pure EVOH	-	-	20.34
1 wt%	1.93	4.56	20.56
3 wt%	2.67	3.31	20.45
5 wt%	2.73	3.24	20.44
7 wt%	2.66	3.32	20.42

APPENDIX C

Inorganic Content of Clay and Organoclays

Table C.1 Inorganic content of clay and organoclays

	Inorganic Content (wt%)
MMT	86.54
MMT_C18/2	67.95
MMT_T	63.32
MMT_2HT	50.13
MMT_C12/15	55.17
MMT_C18/15	50.72



สถาบันวิทยบริการ
จุฬาลงกรณ์มหาวิทยาลัย

APPENDIX D

Inorganic Content of EVOH/Clay Nanocomposite Films at Different MMT_T Organoclay Loading

Table D.1 Inorganic content of EVOH/clay nanocomposite films containing different MMT_T organoclay loading

EVOH_T nanocomposite films	
Organoclay Loading (MMT_T)	Inorganic Content (wt%)
1 wt%	0.61
3 wt%	1.58
5 wt%	2.67
7 wt%	4.06

APPENDIX E

The Crystalline-Melting Temperature (T_m) and The Crystallization Temperature (T_c)

Table E.1 The crystalline-melting temperature (T_m) of EVOH/clay nanocomposite films containing 3 wt% organoclay, which was treated by different surfactants.

	Heating scan (10°C/min)	
	T_m (°C)	ΔH (J/g)
Pure EVOH	163.66	72.9026
EVOH_C12/2	164.13	64.7498
EVOH_C18/2	164.15	68.5619
EVOH_T	163.18	69.5710
EVOH_2HT	163.40	73.1538
EVOH_C12/15	163.96	68.6431
EVOH_C18/15	164.14	72.8209

Table E.2 The crystallization temperature (T_c) of EVOH/clay nanocomposite films containing 3 wt% organoclays, which was treated by different surfactants.

	T_c (°C)		
	Rate of cooling		
	5°C/min	10°C/min	20°C/min
Pure EVOH	148.10	146.48	144.30
EVOH_C12/2	148.48	146.95	144.63
EVOH_C18/2	148.57	146.96	145.04
EVOH_T	147.93	146.27	143.91
EVOH_2HT	148.10	146.18	143.95
EVOH_C12/15	148.71	147.08	144.93
EVOH_C18/15	148.66	147.25	144.93

Table E.3 T_m and T_c of EVOH/clay nanocomposite films containing different MMT_T organoclay loading

EVOH_T nanocomposite films					
MMT_T organoclay loading	T_m (°C)		T_c (°C)		
	Heating rate = 10°C/min		Cooling rate		
	T_m (°C)	ΔH (J/g)	5°C/min	10°C/min	20°C/min
0%	163.66	72.9026	148.10	146.48	144.30
1%	163.64	72.5641	149.37	146.73	144.25
3%	163.18	69.5710	147.93	146.27	143.91
5%	163.35	66.8301	147.33	145.81	143.54
7%	163.19	63.4541	147.02	145.31	143.15

สถาบันวิทยบริการ
จุฬาลงกรณ์มหาวิทยาลัย

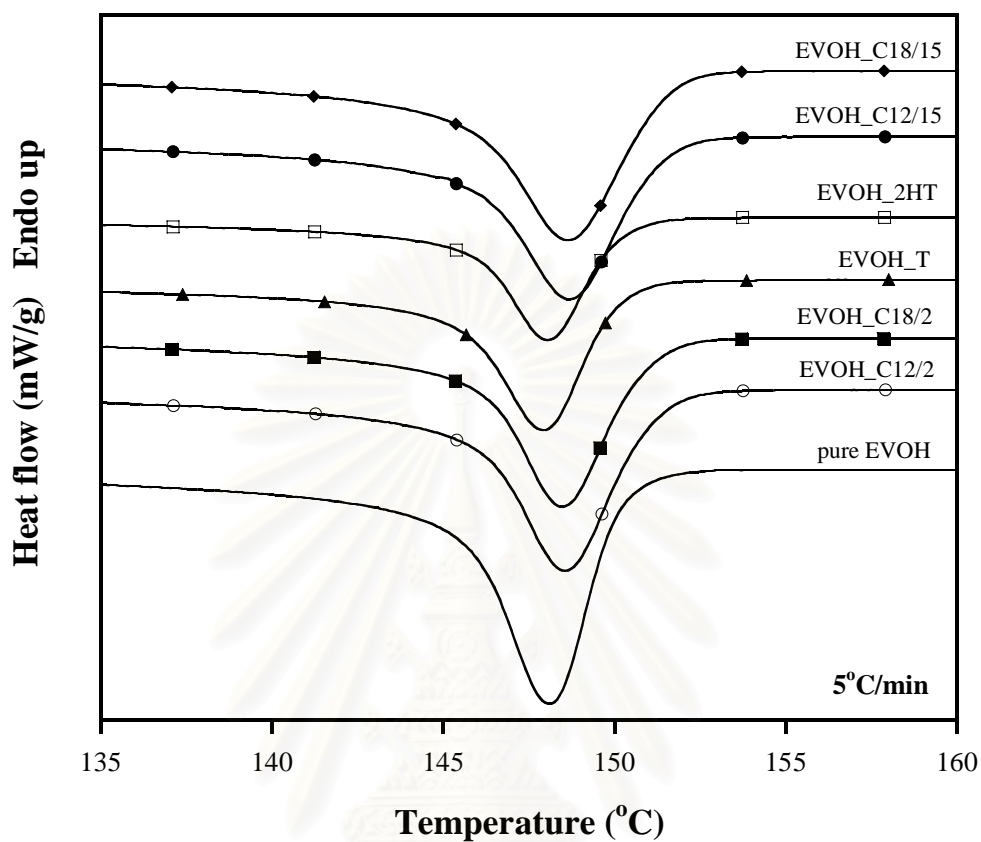


Figure E.1 DSC cooling curves of EVOH/clay nanocomposite films containing 3 wt% organoclays, which were treated with different surfactants, at cooling rate 5°C/min.

สถาบันวิทยบริการ
จุฬาลงกรณ์มหาวิทยาลัย

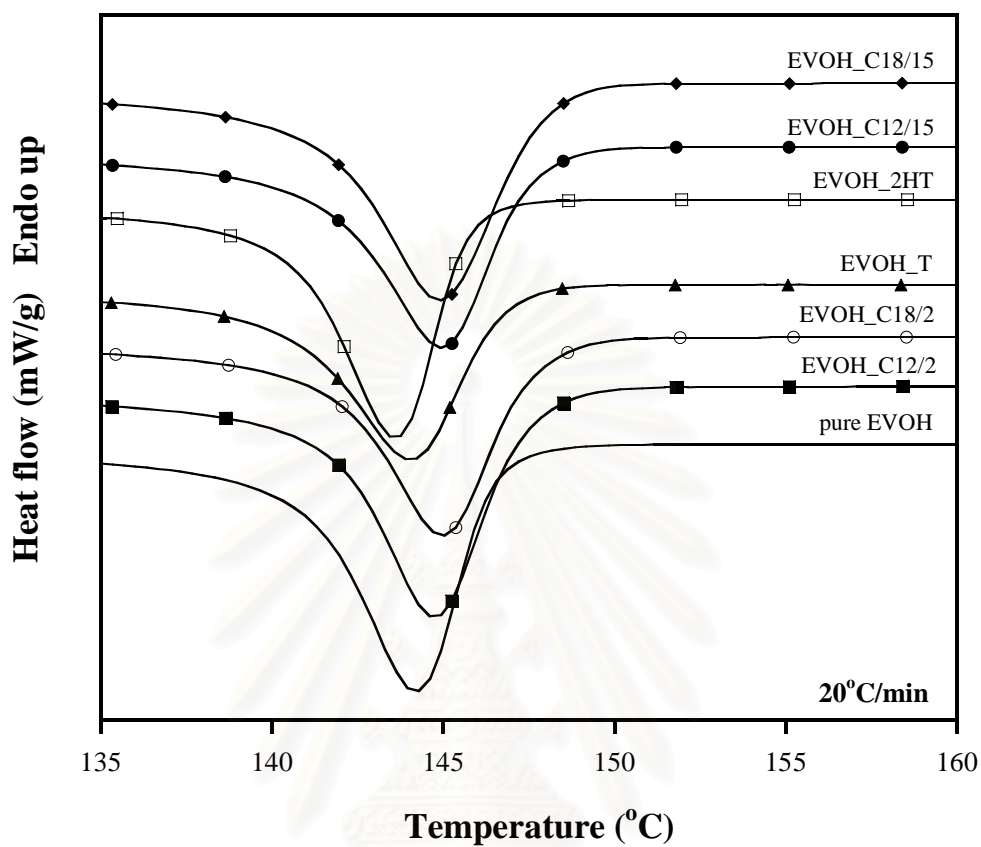


Figure E.2 DSC cooling curves of EVOH/clay nanocomposite films containing 3 wt% organoclays, which were treated with different surfactants, at cooling rate 20°C/min.

สถาบันวิทยบริการ
จุฬาลงกรณ์มหาวิทยาลัย

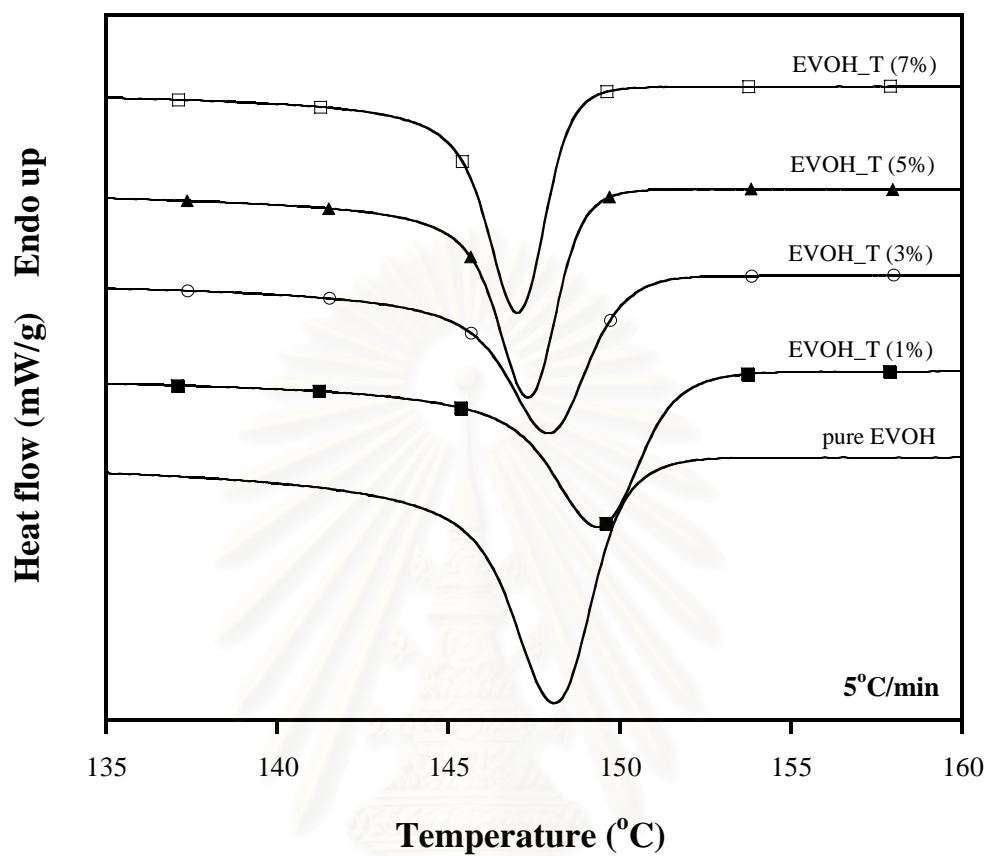


Figure E.3 DSC cooling curves of EVOH/clay nanocomposite films containing different MMT_T organoclay loading, at cooling rate 5°C/min.

สถาบันวิทยบริการ
จุฬาลงกรณ์มหาวิทยาลัย

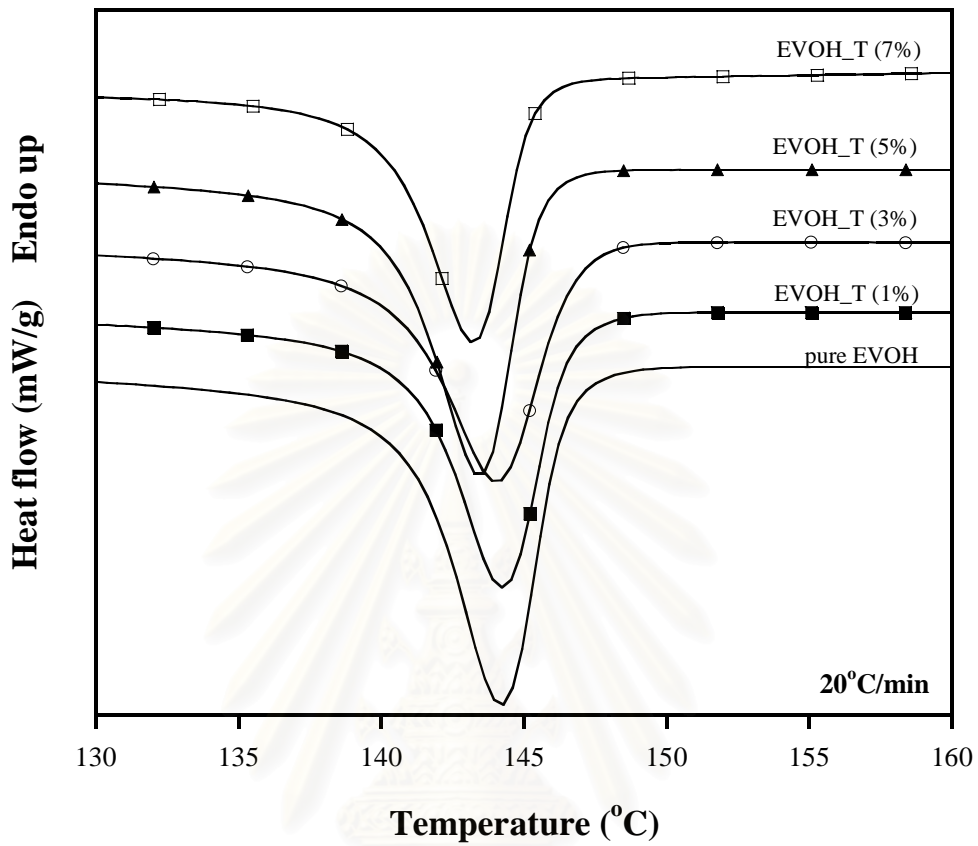


Figure E.4 DSC cooling curves of EVOH/clay nanocomposite films containing different MMT_T organoclay loading, at cooling rate 20°C/min.

APPENDIX F

Percent of Crystallinity Calculation

The degree of crystallinity of the sample can be calculated from both the area under the endothermic peak of the DSC heating profile and the area under XRD peak at $2\theta \sim 20.4^\circ$. From DSC profile, the degree of crystallinity was obtained from the area of the endothermic peak of the film which was determined by the melting enthalpy (ΔH_f) compared to 100% crystalline sample ($\Delta H_{f,100\%}$). The crystallinity of sample is given by the equation [21]:

$$a = \frac{\Delta H_f}{\Delta H_{f,100\%}} \times 100\%$$

where a = The percent of crystallinity of sample (%)

ΔH_f = The melting enthalpy of sample

$\Delta H_{f,100\%}$ = The melting enthalpy of 100% crystalline sample

In this study, because the theoretical value of melting enthalpy of 100% crystalline EVOH can not be obtained, the degree of crystallinity was determined as shown below

$$\Delta C = \frac{\Delta H_{f,nanocomposite}}{\Delta H_{f,pure EVOH}}$$

Where ΔC = The ratio between percent of crystallinity of EVOH/clay nanocomposite films and percent of crystallinity of pure EVOH which was called “The relative degree of crystallinity”

$\Delta H_{f,nanocomposite}$ = The percent of crystallinity of sample (J/g)

$\Delta H_{f,pure EVOH}$ = The percent of crystallinity of pure EVOH (J/g)

For example, the value of melting enthalpy of EVOH/clay nanocomposite films containing 1 wt% MMT_T is 72.5641 J/g. The relative degree of crystallinity (ΔC) can be calculated as follow:

$$\Delta C = \frac{72.5641}{72.9026} = 0.9954$$

Another way to determine the degree of crystallinity of sample is using the area under XRD peak at $2\theta \sim 20.4^\circ$ which is corresponding to the crystalline peak of EVOH. In this study, the degree of crystallinity was determined as shown below

$$\Delta C = \frac{\text{area under peak}_{\text{nanocomposite}}}{\text{area under peak}_{\text{pure EVOH}}}$$

Where ΔC = The ratio between area under XRD peak of EVOH/clay nanocomposite films and area under XRD peak of pure EVOH which was called “The relative degree of crystallinity”

area under peak_{nanocomposite} = The area under XRD peak of sample (J/g) at $2\theta \sim 20.4^\circ$
 area under peak_{pure EVOH} = The area under XRD peak of pure EVOH (J/g) at $2\theta \sim 20.4^\circ$

For example, the area under XRD peak of EVOH/clay nanocomposite films containing 1 wt% MMT_T at $2\theta \sim 20.4^\circ$ is 11.82. The relative degree of crystallinity (ΔC) can be calculated as follow:

$$\Delta C = \frac{11.82}{31.67} = 0.3732$$

Table F.1 The relative degree of crystallinity of EVOH/clay nanocomposite films containing different surfactants, which were determined by XRD.

The relative degree of crystallinity		
	Area under XRD peak	ΔC
Pure EVOH	31.67	1
EVOH_C12/2	17.62	0.5564
EVOH_C18/2	35.23	1.1124
EVOH_T	57.79	1.8248
EVOH_2HT	36.35	1.1478
EVOH_C12/15	19.31	0.6097
EVOH_C18/15	27.99	0.8838

Table F.2 The relative degree of crystallinity of EVOH/clay nanocomposite films containing different MMT_T organoclay loadings, which were determined by XRD.

The relative degree of crystallinity of EVOH_T nanocomposite films		
MMT_T loading	Area under XRD peak	ΔC
0%	31.67	1
1%	11.82	0.3732
3%	30.53	0.9640
5%	37.04	1.1696
7%	34.71	1.0960

Table F.3 The relative degree of crystallinity of EVOH/clay nanocomposite films containing different surfactants, which were determined by DSC.

The relative degree of crystallinity		
	ΔH (J/g)	ΔC
Pure EVOH	72.9026	1
EVOH_C12/2	64.7498	0.8882
EVOH_C18/2	68.5619	0.9405
EVOH_T	69.5710	0.9543
EVOH_2HT	73.1538	1.0034
EVOH_C12/15	68.6431	0.9416
EVOH_C18/15	72.8209	0.9989

Table F.4 The relative degree of crystallinity of EVOH/clay nanocomposite films containing different MMT_T organoclay loadings, which were determined by DSC.

The relative degree of crystallinity of EVOH_T nanocomposite films		
MMT_T loading	ΔH (J/g)	ΔC
0%	72.9026	1
1%	72.5641	0.9954
3%	69.5710	0.9543
5%	66.8301	0.9167
7%	63.4541	0.8704

APPENDIX G

The mechanical properties of EVOH/clay nanocomposites

Table G.1 Tensile strength of pure EVOH

	Tensile Strength (MPa)	Elongation at break (%)	Tensile modulus (GPa)
1	40.53	162.17	1.64
2	39.73	161.25	1.76
3	39.20	146.33	1.65
4	41.39	200.83	1.64
5	38.73	206.00	1.83
6	36.34	117.42	1.64
7	38.77	155.50	1.78
8	39.92	198.42	1.74
9	38.30	138.25	1.66
10	41.16	195.25	1.76
11	39.05	198.00	1.82
12	35.93	113.17	1.70
13	41.69	162.92	1.79
14	36.52	157.42	1.66
15	36.33	176.08	1.67
16	38.60	156.58	1.74
17	37.22	102.33	1.68
18	37.97	123.83	1.74
19	36.82	136.17	1.59
20	36.34	126.75	1.67
Avg.	38.53	156.73	1.71
SD	1.83	31.64	0.07

Table G.2 Tensile strength of EVOH/clay nanocomposite films containing 3 wt%
MMT_C12/2 organoclay

	Tensile Strength (MPa)	Elongation at break (%)	Tensile modulus (GPa)
1	22.71	174.92	1.06
2	21.64	141.08	0.98
3	24.07	198.33	1.09
4	22.68	172.83	1.04
5	19.60	190.92	0.84
6	22.73	209.00	0.96
7	22.85	161.17	1.05
8	21.45	150.00	1.00
9	22.17	158.83	1.37
10	24.76	183.42	1.13
11	25.19	161.75	1.20
12	23.30	102.75	1.07
13	25.66	182.33	1.11
14	25.73	199.83	1.19
15	22.00	181.42	0.99
16	21.85	165.23	1.01
17	37.01	205.42	1.61
18	30.67	119.17	1.45
19	36.19	160.75	1.74
20	30.81	134.25	1.45
Avg.	25.15	167.67	1.15
SD	4.81	28.37	0.23

Table G.3 Tensile strength of EVOH/clay nanocomposite films containing 3 wt%
MMT_C18/2 organoclay

	Tensile Strength (MPa)	Elongation at break (%)	Tensile modulus (GPa)
1	43.85	257.42	1.82
2	42.90	234.67	1.85
3	44.14	239.75	1.84
4	43.98	260.75	1.82
5	42.35	204.33	1.93
6	50.31	214.00	2.41
7	48.80	206.83	2.42
8	42.81	170.42	2.10
9	50.21	203.58	2.40
10	52.06	151.67	2.47
11	51.13	215.42	2.08
12	45.81	176.67	2.20
13	46.89	159.58	2.28
14	43.33	156.83	2.09
15	46.94	190.08	2.30
16	54.16	173.67	2.58
17	46.59	200.50	2.28
18	54.63	143.08	2.73
19	53.11	232.58	2.54
20	50.52	212.75	2.53
Avg.	47.73	200.23	2.23
SD	4.07	34.63	0.28

Table G.4 Tensile strength of EVOH/clay nanocomposite films containing 3 wt%
MMT_2HT organoclay

	Tensile Strength (MPa)	Elongation at break (%)	Tensile modulus (GPa)
1	45.77	122.42	2.20
2	48.26	194.33	2.20
3	48.42	163.92	2.36
4	50.85	167.42	2.42
5	44.80	141.50	2.27
6	47.05	114.58	2.24
7	46.27	151.75	2.10
8	49.51	151.58	2.41
9	52.25	192.25	2.28
10	48.75	144.50	2.27
11	49.43	149.58	2.42
12	55.49	180.75	2.48
13	49.41	173.17	2.23
14	52.38	144.58	2.50
15	51.19	160.78	2.30
16	44.09	145.67	2.12
17	47.58	174.58	2.03
18	48.39	170.83	2.10
19	47.50	144.08	2.82
20	48.08	171.75	2.21
Avg.	48.77	158.00	2.27
SD	2.73	20.88	0.13

Table G.5 Tensile strength of EVOH/clay nanocomposite films containing 3 wt%
MMT_C12/15 organoclay

	Tensile Strength (MPa)	Elongation at break (%)	Tensile modulus (GPa)
1	32.83	103.17	1.52
2	35.06	165.58	1.70
3	35.52	196.50	1.54
4	33.00	123.50	1.53
5	38.53	166.25	1.89
6	30.58	110.58	1.45
7	32.21	114.08	1.60
8	35.85	149.25	1.73
9	35.06	193.33	1.55
10	33.57	169.00	1.56
11	37.70	168.33	1.74
12	33.05	126.92	1.54
13	34.59	121.25	1.65
14	36.33	167.00	1.76
15	34.94	182.67	1.61
16	36.68	169.50	1.75
17	37.21	173.42	1.71
18	40.80	198.75	1.76
19	35.31	100.33	1.73
20	36.12	155.50	1.74
Avg.	35.25	152.75	1.65
SD	2.36	31.91	0.11

Table G.6 Tensile strength of EVOH/clay nanocomposite films containing 3 wt%
MMT_C18/15 organoclay

	Tensile Strength (MPa)	Elongation at break (%)	Tensile modulus (GPa)
1	43.60	116.75	2.16
2	41.64	72.25	1.99
3	37.50	107.83	1.81
4	42.77	94.92	2.12
5	41.53	116.50	2.05
6	39.36	78.67	1.94
7	41.83	72.33	2.06
8	41.18	94.92	2.04
9	39.60	95.92	2.00
10	41.73	130.83	1.90
11	39.95	128.25	1.95
12	43.04	121.92	2.06
13	42.58	136.50	2.06
14	41.33	78.33	2.04
15	43.08	142.50	2.06
16	44.37	141.58	2.08
17	40.20	122.00	2.31
18	41.63	93.67	2.08
19	39.93	127.50	1.92
20	44.41	110.50	2.26
Avg.	41.56	109.18	2.03
SD	1.77	22.88	1.00

Table G.7 Tensile strength of EVOH/clay nanocomposite films containing
1 wt% MMT_T organoclay

	Tensile Strength (MPa)	Elongation at break (%)	Tensile modulus (GPa)
1	42.00	164.25	1.77
2	41.71	137.42	1.91
3	42.15	158.58	1.89
4	49.93	215.25	2.04
5	45.20	201.67	1.88
6	44.59	143.67	2.08
7	47.75	236.25	1.65
8	50.20	260.00	1.73
9	49.94	246.58	1.75
10	45.44	219.92	1.57
11	37.09	163.50	1.50
12	42.94	151.00	1.87
13	63.49	311.00	2.13
14	54.40	324.00	1.61
15	49.42	250.92	1.79
16	49.74	295.42	1.48
17	50.03	263.17	1.72
18	54.83	276.83	1.94
19	47.03	255.25	1.79
20	44.02	181.67	1.80
Avg.	47.60	222.82	1.80
SD	5.82	57.95	0.18

Table G.8 Tensile strength of EVOH/clay nanocomposite films containing
3 wt% MMT_T organoclay

	Tensile Strength (MPa)	Elongation at break (%)	Tensile modulus (GPa)
1	58.84	226.17	2.66
2	57.88	218.00	2.71
3	60.76	260.17	2.32
4	58.37	225.67	2.64
5	67.41	194.92	2.93
6	52.38	196.08	2.31
7	54.63	185.42	2.37
8	55.69	180.42	2.59
9	56.25	170.67	2.61
10	60.12	216.58	2.88
11	63.07	273.33	2.78
12	62.52	222.50	2.78
13	62.17	207.17	2.68
14	57.14	210.75	2.60
15	56.08	201.58	2.34
16	53.10	197.33	2.64
17	59.81	208.50	2.34
18	53.85	195.21	2.61
19	57.70	226.67	2.58
20	55.91	221.75	2.63
Avg.	58.18	211.94	2.59
SD	3.76	24.65	0.01

Table G.9 Tensile strength of EVOH/clay nanocomposite films containing
5 wt% MMT_T organoclay

	Tensile Strength (MPa)	Elongation at break (%)	Tensile modulus (GPa)
1	53.17	227.25	2.15
2	53.71	227.42	2.16
3	55.59	240.08	2.02
4	57.94	266.58	1.95
5	52.41	216.83	1.98
6	53.56	248.17	1.84
7	44.87	173.67	2.21
8	68.74	278.33	2.95
9	54.82	193.25	2.86
10	54.36	185.00	2.95
11	61.88	234.00	3.03
12	47.53	166.50	2.48
13	50.77	190.58	2.39
14	63.48	254.83	2.93
15	51.75	182.25	2.76
16	53.33	166.58	2.74
17	53.62	183.50	2.72
18	53.20	166.58	2.81
19	56.82	188.58	3.00
20	51.46	189.33	2.67
Avg.	54.65	208.97	2.53
SD	5.33	35.59	0.40

Table G.10 Tensile strength of EVOH/clay nanocomposite films containing
7 wt% MMT_T organoclay

	Tensile Strength (MPa)	Elongation at break (%)	Tensile modulus (GPa)
1	45.51	206.50	1.81
2	42.08	108.92	2.01
3	42.45	169.08	1.82
4	34.86	107.75	1.58
5	53.14	237.42	2.10
6	45.95	177.00	2.01
7	44.27	163.08	1.82
8	60.67	258.50	2.22
9	47.06	177.42	2.06
10	39.91	149.08	1.78
11	51.96	222.58	1.99
12	43.30	120.00	2.06
13	53.27	236.75	2.02
14	40.20	124.92	1.87
15	56.53	234.67	2.04
16	37.78	120.00	1.72
17	52.65	217.67	2.25
18	37.41	116.75	1.71
19	51.88	207.58	2.10
20	37.24	72.33	1.84
Avg.	45.91	171.40	1.94
SD	7.24	54.46	0.18

APPENDIX H

The Oxygen Transmission Rate (O₂TR) of EVOH/Clay Nanocomposite Films

Table H.1 Oxygen transmission rate of EVOH/clay nanocomposite films containing 3 wt% organoclays, which were treated with different surfactants, at 23°C, 1 atm and 0 % RH.

	O ₂ TR (cc.mil/m ² .day.atm)
pure EVOH	1.8243
EVOH_C12/2	4.4605
EVOH_C18/2	3.3424
EVOH_C12/15	2.6270
EVOH_C18/15	2.8886
EVOH_T	N/A
EVOH_2HT	1.7770

Table H.2 Oxygen transmission rate of EVOH/clay nanocomposite films containing different MMT_T organoclay loading, at 23°C, 1 atm and 0 % RH.

	O ₂ TR (cc.mil/m ² .day.atm)
EVOH_T (1%)	2.1965
EVOH_T (3%)	N/A
EVOH_T (5%)	3.8294
EVOH_T (7%)	3.7255

VIVAE

Miss.Khamkaew Photyotin was born in Nonthaburi, Thailand on April 28, 1983. She completed senior high school at Pakkred Secondary School, Thailand in 2001 and received Bachelor degree from the Department of Chemical Engineering, Faculty of Engineering, King Mongkut's Institute of Technology Ladkrabang, Thailand in 2005. She continued her study for Master degree at Department of Chemical Engineering, Faculty of Engineering, Chulalongkorn University Bangkok, Thailand.



สถาบันวิทยบริการ
จุฬาลงกรณ์มหาวิทยาลัย